[American Journal of Science, Vol. 307, January, 2007, P. 265–310, DOI 10.2475/01.2007.08]

PETROGENESIS OF THE ULTRAPOTASSIC LINCOLN SYENITE, MAINE: LATE SILURIAN-EARLY DEVONIAN MELTING OF A SOURCE REGION MODIFIED BY SUBDUCTION DRIVEN METASOMATISM

DAVID P. WEST, JR.*†, PAUL B. TOMASCAK**, RAYMOND A. COISH*, MARTIN G. YATES***, and MICHAEL J. REILLY*

ABSTRACT. The Late Silurian-Early Devonian (418 ± 1 Ma) Lincoln syenite, exposed discontinuously over a distance of 75 kilometers in south-central and mid-coastal Maine, represents one of the most unusual igneous rocks in the Appalachian orogen. Detailed field and petrographic study reveals that most of the exposed syenites have been variably affected by post-magmatic recrystallization. However, a small proportion of the syenites in south-central Maine preserve original igneous minerals and textures and allow for an unobstructed study of the igneous petrogenesis. The syenites are characterized by large dark colored alkali feldspar megacrysts set in a finer grained matrix dominated by alkali feldspar + clinopyroxene + orthopyroxene + biotite + oxides. The rocks are intermediate in terms of SiO_2 content (55–59 wt. %), yet are ultrapotassic (6–7 wt. % K_2O) and relatively primitive in terms of their MgO (Mg# > 67), Cr (> 400 ppm), and Ni (> 150 ppm) concentrations. Additionally, the rocks exhibit large ion lithophile element enrichment relative to the high field strength elements along with elevated concentrations of light rare earth elements (200–300 chondritic abundances). The syenites show limited radiogenic isotopic variability with relatively high initial $^{87}Sr/^{86}Sr$ values (0.707 to 0.710), relatively low initial ε_{Nd} values (-4.8 to -6.7), and initial Pb isotopic compositions characteristic of igneous rocks in central Maine (for example, $^{207}Pb/^{204}Pb$ = 15.577 to 15.639).

The geochemical characteristics of these rocks are most consistent with a model involving the partial melting of a mantle wedge previously metasomatized by subduction derived fluids. Crystallization of this magma was influenced by the presence of significant amounts of water that suppressed plagioclase feldspar crystallization, facilitated the crystallization of Mg-rich biotite, and ultimately resulted in the nucleation and growth of the alkali feldspar megacrysts. Correlation with the geochemically similar Parks Pond pluton in eastern Maine extends the distribution of Late Silurian-Early Devonian ultrapotassic magmatism in Maine to an orogen-parallel distance of over 150 km.

Comparisons with rocks of similar composition in known tectonic environments suggest the Lincoln syenite (and by association the Parks Pond pluton) formed as a result of lithospheric extension superimposed on a sub-continental lithospheric mantle source region previously modified by subduction-driven metasomatism. The timing and structural position of this ultrapotassic magmatism is consistent with a geodynamic model involving slab-break off or the convective removal of lithospheric mantle (delamination) in association with Acadian convergence. Both processes facilitate a brief period of crustal extension and decompression melting of source rocks previously modified by subduction related processes.

INTRODUCTION

Highly porphyritic, potassium-rich mafic syenites of the Lincoln syenite (also know as Lincoln sill and Lincoln shonkinite) in south-central and mid-coastal Maine (fig. 1) have been a petrologic curiosity for decades, and the rocks arguably represent one of the most unusual and distinctive igneous rock types in the entire Appalachian orogen. Surprisingly, these rocks have received little in the way of comprehensive study

*Department of Geology, Middlebury College, Middlebury, Vermont 05753
**Department of Earth Sciences, SUNY-Oswego, Oswego, New York 13126
***Department of Earth Sciences, University of Maine, Orono, Maine 04469
†Corresponding Author:Email: dwest@middlebury.edu

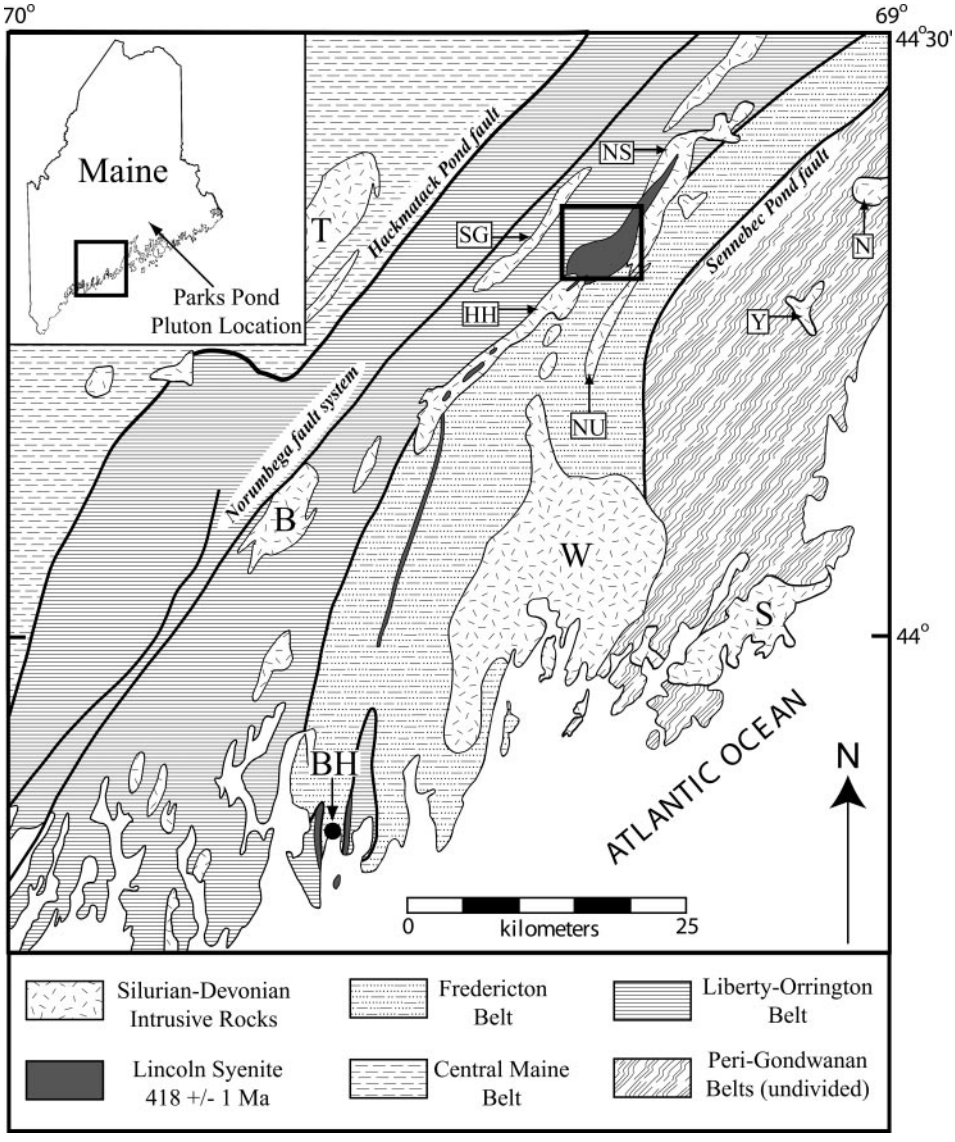

Fig. 1. Generalized geologic map of a portion of south-central and mid-coastal Maine showing the major features discussed in the text (modified from Osberg and others, 1985 and Hussey and Marvinney, 2002). Note the narrow discontinuous exposures of Lincoln syenite south of the main body. The actual widths of these exposures (generally less than 200 meters) have been exaggerated on this map for illustrative purposes. The dark box outlines the approximate area of figure 2. B = Blinn Hill granite (424 ± 2 Ma), HH = Haskell Hill granite (408 ± 5 Ma), N = Northport granite (421 ± 2 Ma), NS = North Searsmont granite gneiss (389 ± 2 Ma), NU = North Union tonalite gneiss(422 ± 2 Ma), S = Spruce Head granite (421 ± 1 Ma), SG = Lake St. George granite gneiss(422 ± 2 Ma), T = Togus granite (378 ± 1 Ma), W = Waldoboro granite (368 ± 2 Ma), Y = Youngtown granite (420 ± 2 Ma); BH = Boothbay Harbor. All quoted ages are U-Pb zircon ages from Tucker and others (2001). The tip of the arrow in the inset map refers to the approximate location of the Parks Pond pluton (discussed later in the text) relative to this figure.

since the work of Trefethen (1937). However, the high potassium, yet mafic to intermediate composition of these igneous rocks provides a unique fingerprint on the tectonic processes responsible for the magma generation and eventual Late Silurian-Early Devonian emplacement (418 ±1 Ma: Tucker and others, 2001) along the eastern margin of the northern Appalachians. Despite intense study, models of Late Silurian-Early Devonian orogenesis (that is, Acadian) in the northern Appalachians remain controversial – in large part due to a paucity of direct evidence for subduction-related processes. Indeed, the words of John Rodgers (1982) ring true nearly 25 years later: "Just what was going on to produce this orogenic episode, climactic for New England and Maritime Canada, is not so certain."

Occurrences of ultrapotassic, mafic to intermediate igneous rocks similar to that of the Lincoln syenite, while rather restricted in the geologic record, are invariably associated with the partial melting of source rocks that have been modified by subduction-related metasomatism (for example, Rogers and others, 1985; Foley and others, 1987; Stolz and others, 1988; Wilson, 1989). However, in studies of active or Cenozoic examples, potassic magma generation may be synchronous with subduction as is the case in Indonesia (Edwards and others, 1991; Gertisser and Keller, 2003) and western Mexico (Carmichael and others, 1996), or it may involve post-subduction melting due to extension (Conticelli and Peccerillo, 1992), delamination (Farmer and others, 2002; Williams and others, 2004), slab roll back (O'Brien and others, 1995), or strike-slip faulting (Sloman, 1989; Vaughan and Scarrow, 2003). While many of these processes have been proposed to have been operative during Late Silurian-Early Devonian time in the northern Appalachians, subtle differences in trace element signatures and isotopic ratios can often help discriminate among these possibilities. Thus, a detailed geochemical study of the Lincoln syenite provides a unique opportunity to provide an independent constraint on the tectonic setting of the region during this important time interval.

The purpose of this paper is to characterize rocks of the Lincoln syenite through a discussion of field relationships, petrography, mineral compositions, and whole rock major element, trace, and isotope geochemistry. The goal of this detailed study is to unravel the processes responsible for the generation and eventual crystallization of this unique magma. Finally, given that potassium-rich magmas similar to the Lincoln syenite occur in rather restricted tectonic settings worldwide, this data can be used to place important constraints on the Late Silurian-Early Devonian geodynamic environment in northern New England.

The distinctive porphyritic mafic syenites that are the subject of this paper have been referred to in a variety of ways over the years. The term "Lincoln sill", first coined by Trefethen (1937) for outcrops in Lincoln County, is most commonly used in the literature to refer to these rocks. While this term is deeply engrained in the minds of many Appalachian geologists, it is not used here for the following reasons: (1) The northwestern intrusive contact of the main body of the syenite (fig. 2), the only locality where an intrusive relationship has been firmly established, is sharply discordant with both lithologic contacts and structural trends in the surrounding country rocks (West and others, 2003; West, 2004). (2) Syenites along southeastern contact of this larger body, as well as the margins of the smaller bodies to the south, while seemingly concordant with the surrounding rocks, are all strongly foliated suggesting post-crystallization modification of original intrusive relationships. Thus the apparent concordance of much of the intrusion noted by Trefethen (1937) is likely due to superimposed structural processes rather than original intrusive contact relationships. The term "Lincoln shonkinite" (Pankiwskyj, 1976; Tucker and others, 2001) has also been used frequently in reference to these rocks. While there are lithologic and

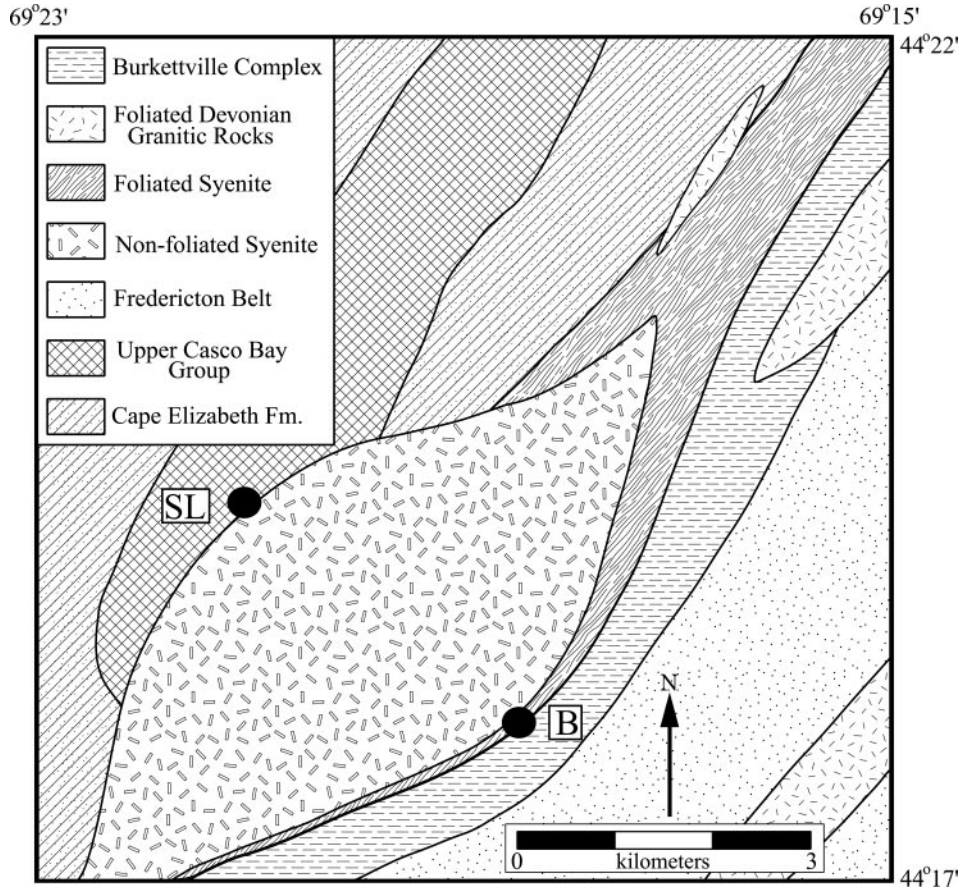

Fig. 2. General geological relationships in the vicinity of the main mass of the Lincoln syenite in south-central Maine. All the analyzed samples, with the exception of MR-44 (an unfoliated sample from the Boothbay Harbor area – see fig. 1), were collected from unfoliated samples within this map area. SL = village of South Liberty and B = village of Burkettville.

geochemical similarities to shonkinitic rocks around the world (to be discussed later), the modal composition of the rocks in Maine do not fit the most recent IUGS definition of shonkinite (that is, they do not contain > 10% foid minerals: Le Maitre, 2002). Modally these rocks are classified as "alkali feldspar syenites" thus, in the interest of brevity; the rocks are herein simply referred to as the Lincoln syenite

PREVIOUS STUDIES

In a paper appropriately titled "Some Unusual Rocks from Maine", Bastin (1906) provided the first formal descriptions of rocks of the Lincoln syenite. In addition to detailed petrographic descriptions of the rocks and a written description of the outcrop pattern in the South Liberty - Burkettville area (fig. 2), a whole rock geochemical analysis was provided. Bastin (1906) recognized the rocks were "peculiar in their high alkali content and in the preponderance of potash over soda." Soon thereafter, Ogilvie (1907) in a discussion of the geology of the Boothbay area (see fig. 1), recognized and described several different varieties of the Lincoln syenite (for

example, foliated and unfoliated) in this region (see fig. 1). In addition to detailed petrographic descriptions, she provided a sketch map showing the distribution of these rocks in the Boothbay area along with several whole rock geochemical analyses. Ogilvie (1907) correlated the syenites in the Boothbay area with those described to the north by Bastin (1906) and she similarly recognized the unusual nature of the whole rock chemistry. In discussing this whole rock chemistry, Ogilvie (1907) noted geochemical similarities with shonkinites in the Bearpaw Mountains of Montana as well as with potassic volcanic rocks in Italy.

Trefethen (1937), in a paper simply titled "The Lincoln Sill," provided the first, and as it turns out, the only comprehensive study of the Lincoln syenite rocks prior to the present work. Trefethen (1937) was the first to coin the term "sill" in reference to these rocks after noting that the contacts of the intrusion were "generally concordant with the structural trend lines of the area." Trefethen's studies focused on the exposures in the South Liberty – Burkettville area (area of fig. 2), and in addition to providing a sketch map of the intrusion in this region, he recognized and provided detailed descriptions of four different rock types (to be discussed below). Trefethen (1937) did not provide any new chemical analyses for the rocks, but he did re-print all the earlier results of Ogilvie (1907) and provided an extensive discussion of these results. Trefethen concluded the unusual rocks of the Lincoln syenite originally formed through a process of hybridization and many of these rocks were subsequently affected by post-magmatic alteration and superimposed metamorphism.

Elders (1969) in an extended abstract provided detailed information on the chemistry of the zoned alkali feldspar megacrysts within the syenite. Elders noted 30 to 40 compositional zones 1 to 2 mm wide within most feldspar megacrysts. Within each of these compositional zones, Elders (1969) noted compositions that ranged from $Or_{55}\,Ab_{45}$ (inner edges) to $Or_{85}\,Ab_{15}$ (outer edges) and these patterns were repeated in an oscillatory fashion. In addition, Elders noted "zonally arranged inclusions of groundmass minerals" within the alkali feldspar megacrysts that he interpreted to reflect the early nucleation of alkali feldspar during magma crystallization.

Pankiwskyj (1976) provided a detailed geologic map of the area underlain by the main body of the Lincoln syenite (area shown in fig. 2) and was the first to apply the term "shonkinite" directly to these rocks. The bedrock geologic map of Maine (Osberg and others, 1985) subsequently provided an overview of the spatial distribution of all the Lincoln syenite rocks in Maine – from Squirrel Island just south of Boothbay Harbor to the wide body of syenite in the South Liberty – Burkettville area.

Knight and Gaudette (1991) provided the first isotopic and geochronological data from the Lincoln syenite. Based on a combination of Rb-Sr analyses (both whole rock and mineral separates) and U-Pb zircon analyses (3 size fractions) a crystallization age of "at or near 386 Ma" was determined. This age should be considered suspect for the following reasons: (1) Some of the samples used in the Rb-Sr analyses were foliated and recrystallized and thus Sr mobility may have influenced the results. Considerable scatter in the Rb-Sr whole rock results (isochron age = 324 ± 53 Ma) would seem to justify this concern. (2) The sample used in the U-Pb zircon analyses was collected from the foliated phase along the eastern margin of the intrusion. Given the extensive recrystallization observed in these rock types it seems possible that some or all of the zircons analyzed grew during this recrystallization episode rather than during original crystallization. (3) The interpreted age of crystallization (386 Ma) age is very similar to $^{40}Ar/^{39}Ar$ hornblende ages (~ 380 Ma) north of the intrusion (West and others, 1995). These hornblende ages are interpreted to date cooling following metamorphism in the area and thus the coincidence of the Knight and Gaudette (1991) Lincoln syenite age with these metamorphic cooling ages is suspicious. (4) Finally, Tucker and

others (2001) report a high-precision U-Pb zircon age of 418 ± 1 Ma (weighted mean of 4 concordant analyses) from the non-foliated phase of the Lincoln syenite. Thus, given all the factors discussed above, the 386 Ma age of Knight and Gaudette (1991) is likely an approximation of the timing of deformation and recrystallization in the Lincoln syenite, while the 418 Ma age of Tucker and others (2001) likely provides the timing of original igneous crystallization.

REGIONAL GEOLOGIC SETTING

Highly porphyritic alkali feldspar syenites are exposed discontinuously over a distance of nearly 75 kilometers in south-central and mid-coastal Maine (Trefethen, 1937; Osberg and others, 1985; and fig. 1). The bedrock geology of this region is characterized by a number of different lithotectonic sequences that were juxtaposed during Silurian-Devonian orogenesis (Berry and Osberg, 1989; Tucker and others, 2001). All of the stratified rocks within the area of figure 1 have been multiply deformed, metamorphosed to amphibolite facies, and intruded by several generations of plutonic rocks. The interested reader is referred to Tucker and others (2001) for an overview of the geologic relationships in the northern half of figure 1 and Hussey and Berry (2002) should be consulted for an overview of the geology in the southern half.

Rocks of the Lincoln syenite have been mapped within two lithotectonic sequences in Maine: (1) Ordovician rocks of the Liberty-Orrington belt in south-central Maine (Pankiwskyj, 1976; West, 2004) and (2) latest Ordovician to Silurian rocks of the Fredericton belt in mid-coastal Maine (Osberg and others, 1985; Hussey and Marvinney, 2002). The Liberty-Orrington belt has been interpreted to represent a complex sequence of metamorphosed arc to back-arc igneous and sedimentary rocks that formed outboard of the Laurentian margin (that is, peri-Gondwanan) in Middle to Late Ordovician time (West and others, 2004). The Fredericton belt is composed of calcareous and pelitic meta-sedimentary rocks that were originally deposited along the Laurentian margin in latest Ordovician to Silurian time (Ludman and others, 1993).

Numerous intrusive rock bodies of somewhat similar age but dissimilar composition are exposed in the vicinity of the Lincoln syenite. In particular, the slightly older and strongly deformed Lake St. George granite gneiss and North Union tonalitic gneiss (both 422 ± 2 Ma: Tucker and others, 2001) are exposed to the northwest and southeast, respectively, of the main body of the Lincoln syenite (fig. 1). It should also be noted that the regionally extensive coastal Maine magmatic province (Hogan and Sinha, 1989) is located to the east and northeast of the Lincoln syenite (east of the Sennebec Pond fault on fig. 1). Many of the plutons within this province are Late Silurian in age including the Spruce Head (Ayuso and Arth, 1997), Youngtown, and Northport intrusions shown on figure 1. Most of the Late Silurian plutons in this magmatic province are bimodal in composition and show evidence of mafic and felsic magma mingling (Stewart and others, 1988; Hogan and Sinha, 1989; Wiebe, 1993, 1994; Seaman and others, 1995; Ayuso and Arth, 1997; Wiebe and others, 2004).

In addition to the slightly older Late Silurian magmatism discussed above, several younger Devonian plutons intrude rocks of the Lincoln syenite (see fig. 1). The Haskell Hill granite gneiss (408 ± 5 Ma: Tucker and others, 2001) is exposed immediately southwest of the main body, while the North Searsmont granite gneiss (389 ± 2 Ma: Tucker and others, 2001) is exposed immediately to the northeast. As the names imply, both of these rock bodies are felsic in composition and have been subjected to extensive deformation and recrystallization. Finally, somewhat larger but considerably younger granitic plutons (~ 370 – 380 Ma) are also exposed in the region (for example, the Waldoboro pluton: Barton and Sidle, 1994).

GEOLOGY OF THE LINCOLN SYENITE

Mapped Geologic Relationships

The regional distribution the Lincoln syenite as portrayed in figure 1 does not deviate significantly from that originally described by Trefethen (1937) and later shown on the bedrock geologic map of Maine (Osberg and others, 1985). The main mass of the intrusion is located between the villages of South Liberty and Burkettville in south-central Maine (fig. 2). In this region the syenite forms a northeast trending lens-shaped body up to 4.5 kilometers wide that underlies an area of approximately 35 km^2 (Pankiwskyj, 1976; West, 2004). The northwestern margin of the intrusion in this region is highly discordant to stratified rocks of the upper Casco Bay Group (West and others, 2003; West, 2004). This northwestern contact is interpreted to be an intrusive contact based on the presence of abundant country rock xenoliths within the syenite near the contact, hornfelsic textures within immediately adjacent country rocks, and isolated occurrences of a narrow chilled margin in the vicinity of the contact (West and others, 2000). In contrast, syenites along the southeastern margin of the intrusion are strongly deformed and recrystallized (see below) and separated from rocks of the Fredericton belt by highly sheared rocks of the Burkettville Complex (West and others 2000; West, 2004). Thus the southeastern contact of the main mass of Lincoln syenite with rocks of the Fredericton belt is interpreted to be tectonic. However, it should be noted that further south rocks of the Lincoln syenite are clearly contained entirely within rocks of the Fredericton belt (see below).

South of the main mass of Lincoln syenite in the South Liberty – Burkettville area, exposures thin dramatically to widths of less than 200 meters and eventually become discontinuous (West and Peterman, 2004; Grover, 2007). In some cases this thinning to the south is due to interruption by younger granitic intrusions (for example, Haskell Hill granite gneiss), but much of it is likely due to superimposed shearing. The narrow isolated bodies of syenite are always foliated and recrystallized, typically more strongly along their margins, and the foliation is parallel with the foliation in the surrounding country rocks. So while the original intrusion likely narrowed to the south, much of the thinning and parallelism with the surrounding country rock structure is due to superimposed deformation.

Further south, in the Boothbay Harbor region (fig. 1), rocks of the Lincoln syenite are folded into two parallel bands and are contained almost entirely within the Bucksport Formation of the Fredericton belt (Hussey and Marvinney, 2002). Although the syenite exposures widen in places along the Boothbay peninsula (up to 500 meters), contacts generally remain parallel to the surrounding country rocks and the margins of the syenite bodies are strongly foliated and recrystallized (Ogilvie, 1907; Hussey and Berry, 2002).

Rock Types

Rocks of the Lincoln syenite are unmistakable in appearance being characterized by large (up to 7 cm in length) generally euhedral dark-colored alkali feldspar megacrysts set in a medium-grained matrix dominated by mafic minerals (figs. 3A-D). Beginning with the earliest accounts (Bastin, 1906; Ogilvie, 1907), both foliated and unfoliated varieties of the syenite have been recognized and described. Trefethen (1937) additionally described a finer grained non-porphyritic variety along the northwestern margin of the intrusion in the South Liberty area (fig. 2). Based on detailed studies in the South Liberty – Burkettville area (fig. 2) and reconnaissance studies further to the south, rocks of the Lincoln syenite are herein divided into four general types: (1) non-foliated, porphyritic, pyroxene-rich alkali feldspar syenite (unaltered phase), (2) nonfoliated, non-porphyritic, olivine-bearing alkali feldspar syenite (bor-

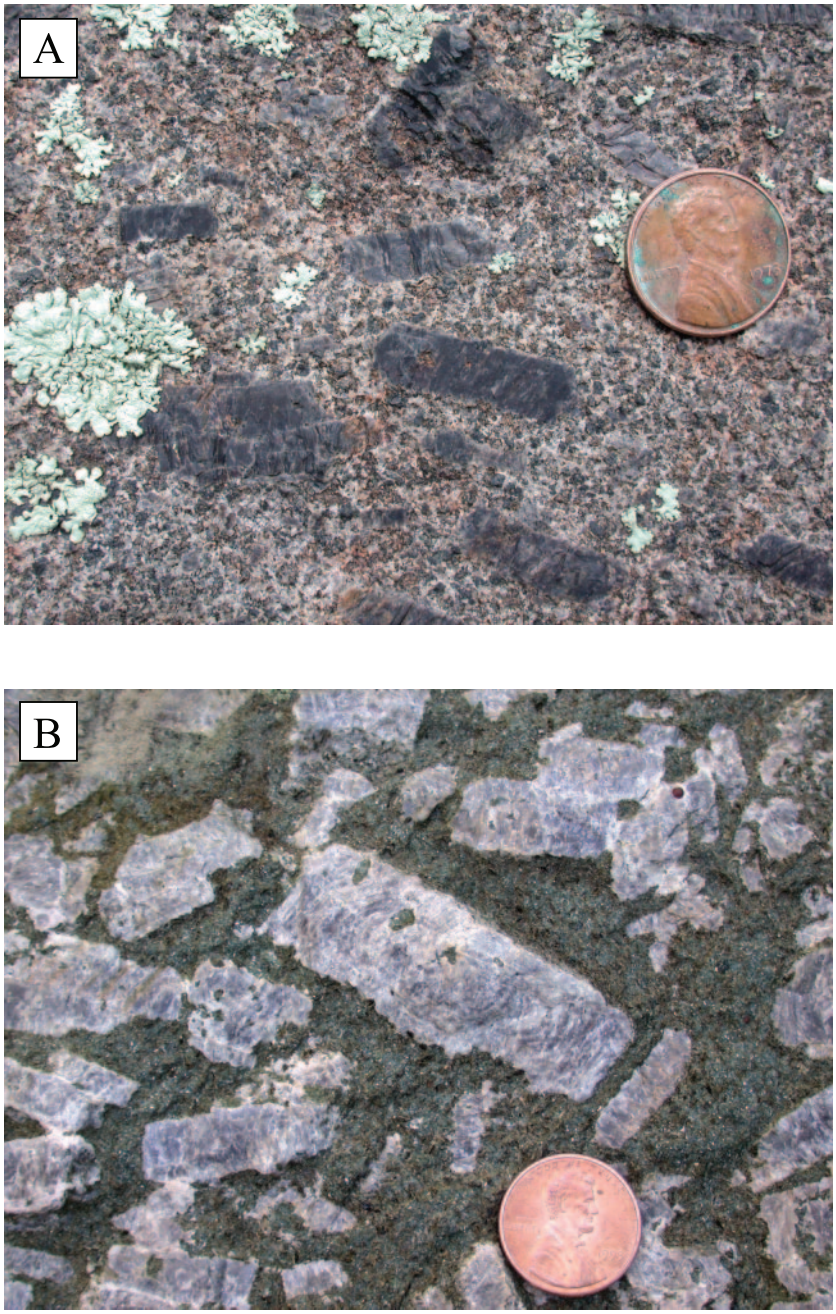

Fig. 3. Photographs showing megascopic textural and structural characteristics of the Lincoln syenite. (A) Unfoliated alkali feldspar syenite that shows no evidence of recrystallization. Note the dark gray alkali feldspar megacrysts set in a finer grained matrix of alkali feldspar, orthopyroxene, clinopyroxene, and biotite. (B) Recrystallized variety of alkali feldspar syenite containing light gray alkali feldspar megacrysts set in a finer grained un-foliated matrix composed primarily of biotite and calcic- amphibole. Note the inclusions of groundmass material within some of the megacrysts.

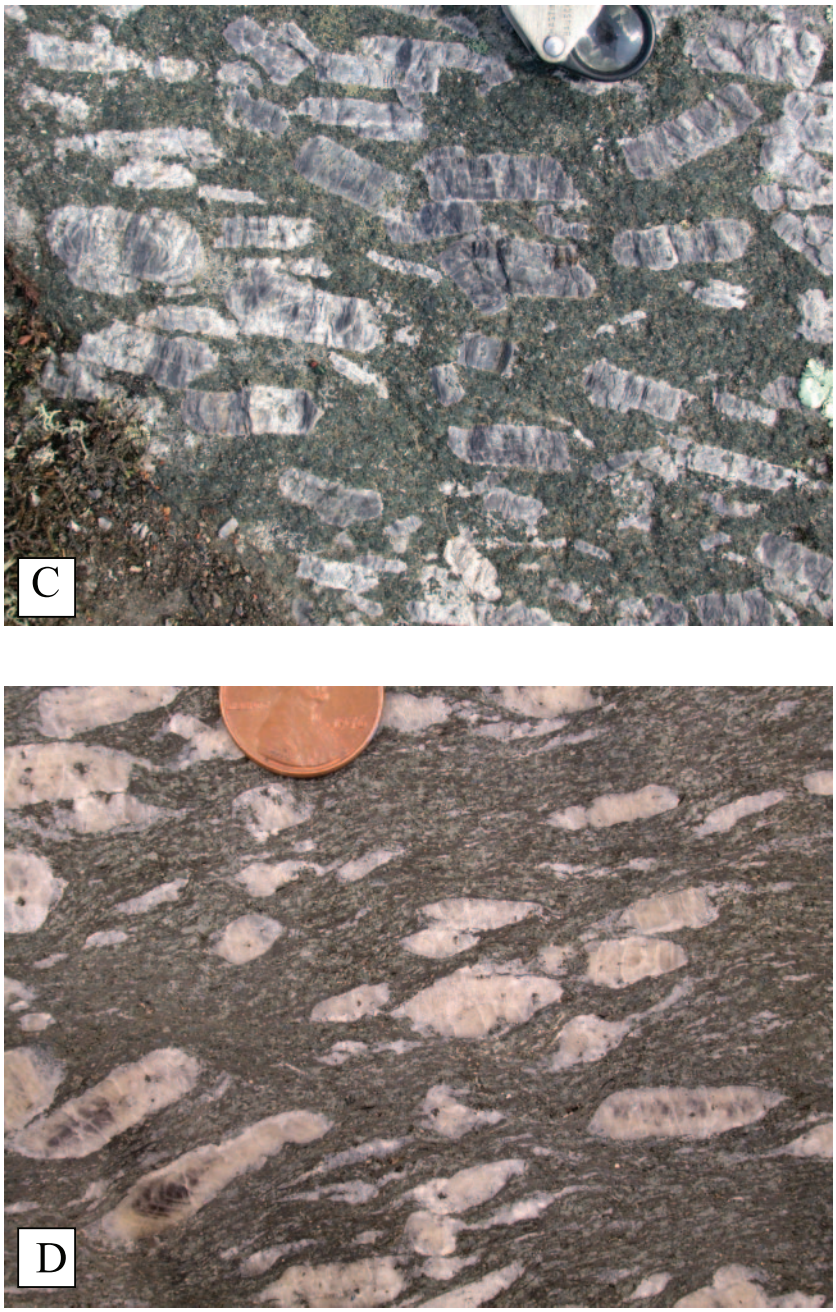

Fig. 3. (C) Parallel alignment of alkali feldspar megacrysts in an unfoliated matrix of biotite and amphibole. This feldspar alignment is interpreted to reflect magmatic flow rather than tectonic stresses. (D) Strongly foliated and recrystallized variety of syenite characteristic of rocks found along the southeastern side of the intrusion. The feldspars are aligned in a matrix of foliated biotite, calcic-amphibole, quartz and feldspar.

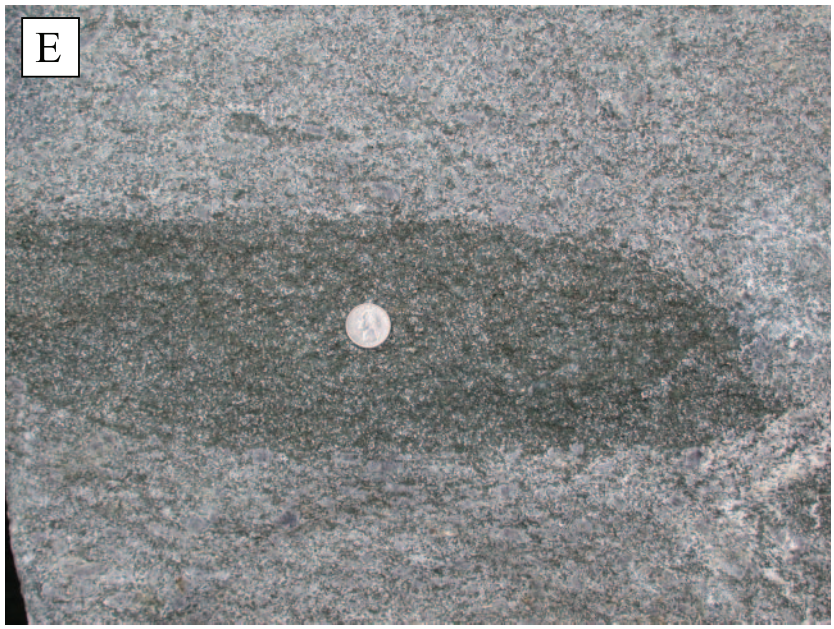

Fig. 3. (E) Rounded mafic enclave within porphyritic alkali feldspar syenite that is mineralogically and texturally similar to the rocks shown in fig. 3A. The enclave has a mineralogy similar to the matrix mineralogy in the syenite, however, this particular enclave contains no alkali feldspar megacrysts.

der phase), (3) non-foliated porphyritic, amphibole-rich alkali feldspar syenite (recrystallized phase), and (4) megacrystic, biotite, amphibole, alkali feldspar schist (deformed and recrystallized phase). Each of these rock types contains abundant biotite as a characteristic accessory mineral. Due to relatively poor exposure and the uneven spatial distribution of the recrystallized phase (rock type 3), only the foliated and recrystallized variety (rock type 4 above) has been mapped separately (West, 2004, and fig. 2).

Non-foliated, porphyritic, pyroxene-rich alkali feldspar syenite (figs.3A and 4A).—These rocks are only found within the northwestern third of the large South Liberty – Burkettville lens and they show no evidence of foliation or recrystallization. The observed minerals and textures are interpreted as igneous in origin. The rocks are characterized by large (average ~ 4 cm, but up to 7 cm in length) euhedral to subhedral dark-gray to purplish-gray alkali feldspar megacrysts set in a medium-grained matrix of biotite, clinopyroxene, orthopyroxene, and alkali feldspar. Quartz and plagioclase feldspar are found in only trace amounts (if at all) in the groundmass. The alkali feldspar megacrysts show modal variability within the intrusion but generally comprise 25 to 50 percent of the rock. These feldspars are often megascopically zoned and in thin section microperthite and oscillatory zoning are evident (fig. 4D). The alkali feldspar megacrysts are typically rich in inclusions that are often concentrated along internal compositional zone boundaries. These inclusions include fine-grained biotite and clinopyroxene (fig. 4D) as well as abundant tiny needle-like (< 1 μm in width and up to 40 μm in length) inclusions that appear to be rutile. As originally suggested by Bastin (1906), the presence of these minute inclusions give the alkali feldspars their unique dark color.

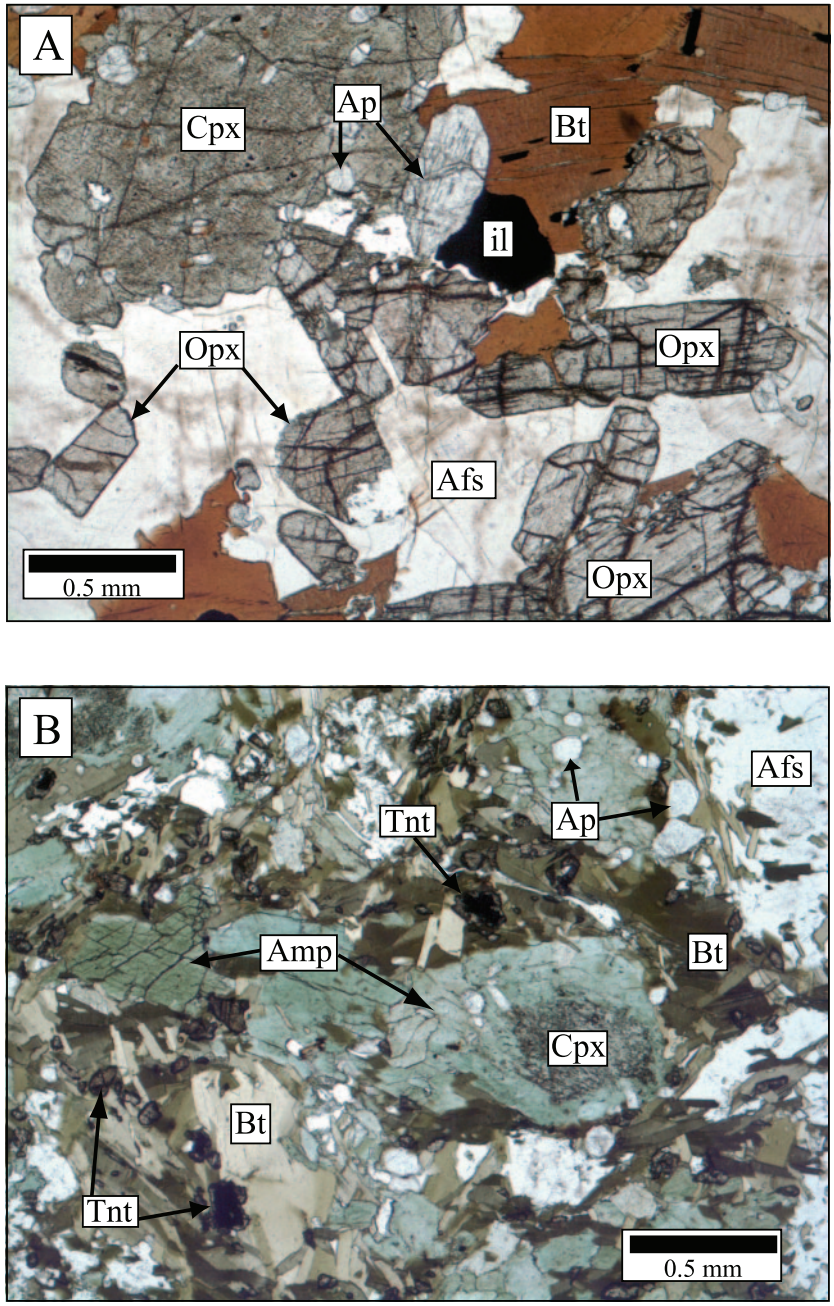

Fig. 4. Photomicrographs in plane polarized light showing textural and mineralogical characteristics of the Lincoln syenite. (A) Typical groundmass mineralogy in unaltered and unfoliated syenites (type 1). Note the euhedral nature of the orthopyroxene, the subhedral and exsolved clinopyroxene, and the interstitial nature of the matrix alkali feldspar and biotite. (B) Typical groundmass mineralogy in the altered but unfoliated syenite (type 3). Note the complete mantling of highly resorbed clinopyroxene by light green calcic amphibole and the presence of titanite commonly containing cores of ilmenite.

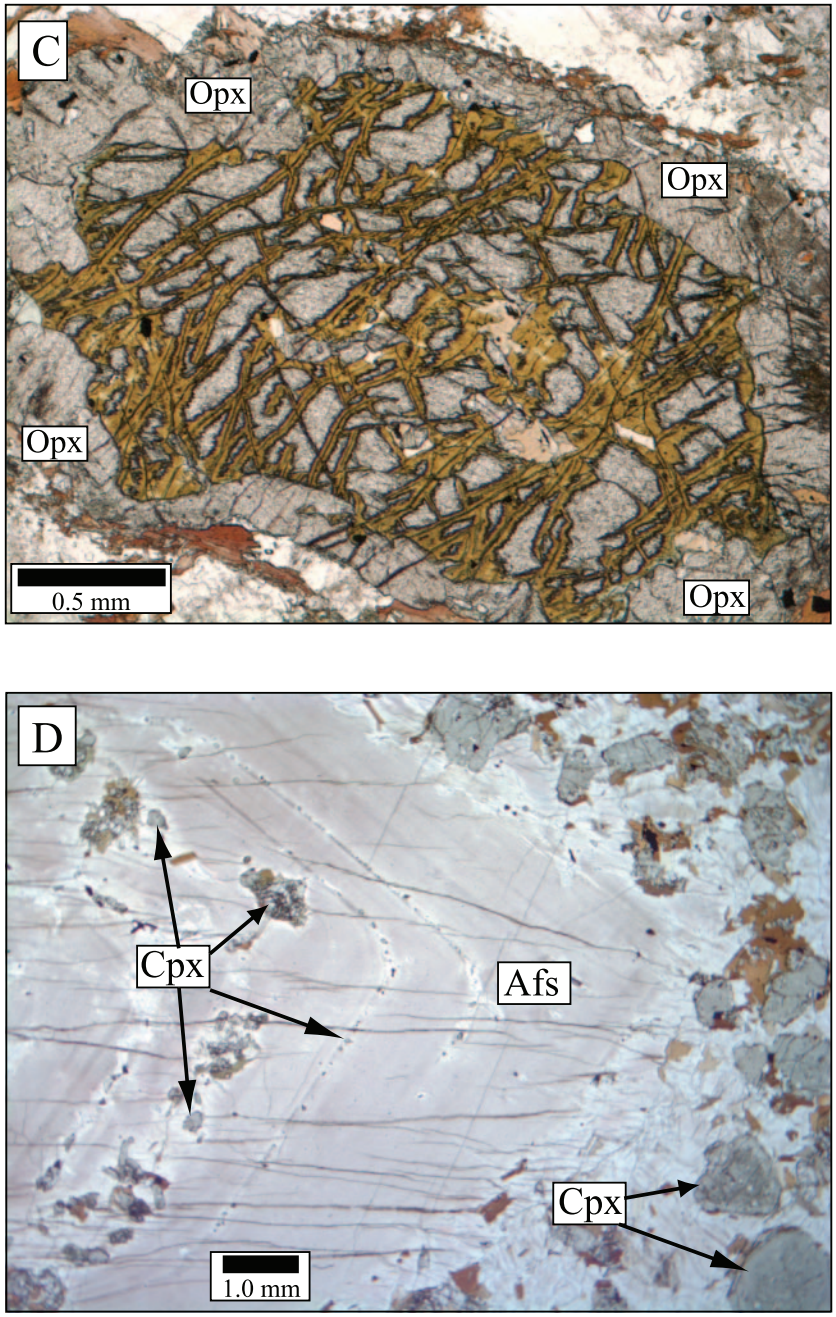

Fig. 4. (C) Non-foliated and non-porphyritic syenite (type 2) showing a core of altered Mg-rich olivine completely mantled by orthopyroxene. (D) Margin of a zoned alkali feldspar megacryst – note the presence of clinopyroxene inclusions concentrated along growth bands within the megacryst. Larger subhedral clinopyroxene is found in the groundmass (right side of the photo) along with biotite and groundmass alkali feldspar.

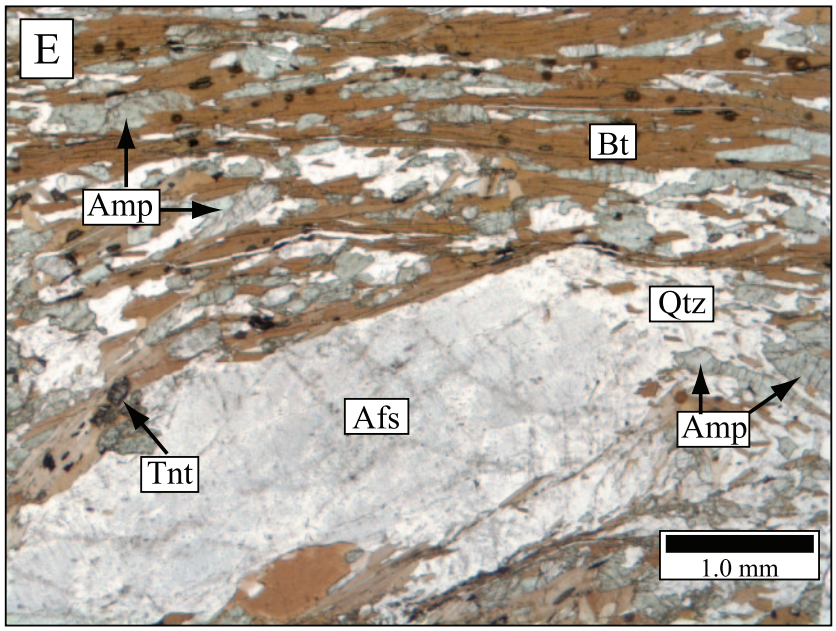

Fig. 4. (E) Typical mineralogy and texture of foliated and recrystallized variety of the syenite (type 4) from the southeastern margin of the intrusion.

Macroscopically, the alkali feldspar megacrysts of this phase show varying degrees of preferred alignment. In some exposures, megacrysts show no apparent alignment, however, in many other outcrops the megacrysts do indeed exhibit a distinct parallel alignment (fig. 3C). The general orientation of this alignment is highly variable, both within an individual outcrop and within the intrusion as a whole. Unfortunately, a paucity of three-dimensional outcrops has prevented a quantitative assessment of the feldspar alignment within the intrusion. Given the apparent variability of this alignment and the lack of matrix foliation in these rocks, this alignment is interpreted to reflect magmatic flow rather than post-crystallization tectonic stresses (Trefethen, 1937; this study).

Considerable variability in the modal amounts of individual groundmass minerals occur in this phase. In some rocks the groundmass is rich in interstitial alkali feldspar (up to 40% of the groundmass), while in others alkali feldspar is only a minor constituent (< 5%). Nearly all rocks contain both clino- and orthopyroxene, with clinopyroxene usually, but not always, dominating. Modal amounts of pyroxene in the groundmass range from 30 to 75 percent. Biotite is always present and composes up to 40 percent of the groundmass mineralogy in some cases. Accessory minerals include ilmenite, apatite, and zircon.

Non-foliated, non-porphyritic, olivine-bearing, alkali feldspar syenite (fig. 4C).—These rocks, first noted by Trefethen (1937), have only been found in very isolated localities along the northwestern margin of the South Liberty – Burkettville lens where the intrusive contact is exposed. Although few exposures are available, this rock type appears only to be found within approximately 5 meters of the contact (West and others, 2000). While the rock does contain zoned euhedral to subhedral alkali feldspar phenocrysts up to 5.0 mm in length (< 15% modally), it lacks the large megacrysts so

characteristic of the other rock types. The rock is dominated by (listed in order of decreasing abundance) alkali feldspar, biotite, clinopyroxene and orthopyroxene with the typical grain size being in the 0.5 to 2.5 mm range. Minerals found in minor abundances include quartz, plagioclase feldspar, apatite, zircon, and ilmenite. In addition to these minerals, Mg-rich olivine can occasionally be found in thin section ($< 1\%$ modal abundance). This olivine is partially typically altered (bowlingite) and always completely mantled by orthopyroxene (fig. 4C). Olivine has not been observed at any other localities within the intrusion.

Non-foliated, porphyritic, amphibole-rich alkali feldspar syenite (figs. 3B and 4B).—These rocks, the most common variety of syenite, can be found throughout the South Liberty – Burkettville lens except along the southeastern and northeastern margins where the rocks are foliated. In addition, these rocks can also be found in the interior portions of narrower lenses to the south, particularly on the Boothbay peninsula (Hussey and Berry, 2002). The alkali feldspar megacrysts in this phase are similar in size and texture to those described above. However the groundmass mineralogy is quite different. The groundmass in these rocks is dominated by light green calcic-amphibole and biotite. Quartz and plagioclase feldspar are more common groundmass constituents in this phase, together comprising up to 15 percent of the groundmass in some rocks. In addition to the accessory minerals listed above, titanite is commonly present as a groundmass accessory mineral in this phase.

It is common throughout the length of the syenite to find unfoliated porphyritic syenites that contain pyroxenes rimmed by calcic amphibole and ilmenite rimmed by titanite (Ogilvie, 1907; Trefethen, 1937; Hussey and Berry, 2002; fig. 4B). A complete gradation from amphibole-free syenites (fig. 4B) to syenites containing pyroxenes rimmed to varying degrees by calcic amphibole (fig. 4B), to pyroxene-free syenites (fig. 4C) has been observed. Similarly, when amphibole is present in the groundmass, ilmenite is commonly absent or partially rimmed by titanite (fig. 4B). Thus, it is suggested that the different groundmass mineralogy observed in this phase represents late to post-magmatic recrystallization processes. These reactions were likely driven by the availability of water during the late stages of magma crystallization, or due to the variable introduction of water subsequent to crystallization.

Megacrystic, biotite, amphibole, alkali feldspar schist (figs. 3D and 4E).—Strongly foliated alkali feldspar syenites can be mapped separately along the southeastern and northeastern margins of the South Liberty –Burkettville lens (West, 2004, fig. 2). In addition, these rocks are found extensively along the margins of the narrow lens shaped bodies of syenite to the south (Hussey and Berry, 2002; West and Peterman, 2004; Grover, 2007). The intensity of the foliation varies from highly foliated and strongly sheared rocks along the margins of the intrusion to rather weakly foliated varieties found within the interior zones. Typically the alkali feldspar megacrysts are aligned parallel to the schistosity in the groundmass minerals and the overall trend of this foliation in most cases parallels the foliation in adjacent stratified rocks. This foliation is interpreted to reflect post-magmatic metamorphic recrystallization associated with tectonic deformation.

The alkali feldspar megacrysts preserve many of the distinctive characteristics of the megacrysts in the non-foliated varieties (for example, fine-scaled oscillatory zoning and dark color due to small inclusions) leaving no question as to the protolith. However, in strongly foliated varieties, the feldspars show evidence of extensive mechanical abrasion (fractured grains) and recrystallization along their margins (fig. 4E) that often result in lighter colored alkali feldspar megacrysts (fig. 3D). The matrix of these rocks is dominated by foliated biotite, calcic amphibole and titanite. In addition, fine-grained quartz and plagioclase feldspar is present both with the ground-

mass and along the margins of the sheared alkali feldspar megacrysts. With the exception of the cores of the alkali feldspar megacrysts, all of the minerals in the strongly foliated syenites are interpreted to be the product of metamorphic processes. Pyroxene is not preserved in strongly foliated varieties, and only rarely preserved in moderately to weakly foliated syenites.

Mafic Enclaves (fig. 3E).—Fine-grained mafic enclaves, while not common, do occur within rocks of the Lincoln syenite. Enclaves range in size to up to more than a meter across and all are rounded along their margins. While most enclaves lack the alkali feldspar megacrysts, several have been observed to contain megacrysts along their margins. The enclave mineralogy is similar to the groundmass mineralogy of the enclosing porphyritic syenites.

SAMPLE SELECTION AND ANALYTICAL TECHNIQUES

Because many of the syenites have been subjected to significant post-magmatic recrystallization and deformation, care was taken to only select samples for geochemical analyses that were minimally affected by these processes (that is, samples that contained little to no amphibole). An additional concern with the whole rock geochemistry is the coarse grain size of the alkali feldspar megacrysts and what appears to be the uneven distribution of some of the accessory minerals (for example, zircon). In an attempt to ultimately analyze representative samples from individual localities, large samples (10 to 20 kg) were collected, crushed and split prior to analyses. Finally, efforts were made to sample the complete range of rock types observed, in particular rocks that displayed a range in the modal amounts of alkali feldspar, orthopyroxene, clinopyroxene, and biotite.

Mineral Chemistry

The major element chemistry of minerals was performed on a Cameca SX-100 electron microprobe at the University of Maine using a 15 kV, 10 nA, 5 μm beam and 20 or 40 second counts. Analyses were corrected for matrix effects using the method of Merlet (1992). Simple silicate and oxide standards were used, and calibrations were tested by analyzing these standards as unknowns. Precision for analyses range from less than 0.5 percent for values above 50 weight percent to less than 5 percent for values around 1 weight percent. The data presented in table 1 represents an overview of over a thousand individual analytical points averaged into over 130 mineral analyses.

Chemical and electron backscatter stage maps were collected with a 15kV, 100nA, 20μm defocused beam and 20msec dwell times. The chemical maps were false colored with the NIH ImageJ program. Low Ba concentration in the K-feldspar megacrysts necessitated smoothing the Ba chemical map with a 20μm gaussian blur.

Major and Trace Element Geochemistry

Whole rock samples were crushed in a porcelain jaw crusher and powdered in a tungsten carbide shatterbox. Major elements and Sc, V, Cr, Co, Ni, Cu and Zn were determined on an ICP-OES (Thermal Element IRIS 1000 DUO) at Middlebury College. Samples were fused using $LiBO_2$ flux (Coish and Sinton, 1992) and dissolved in 10 percent HNO_3. Dilute solutions (~500x for traces and ~10,000x for majors) were run on the ICP. Precision for major elements is lower than 3 percent, and for minor and trace elements lower than 6 percent relative. Rb, Sr, Zr, Y, Nb, Ta, Hf, Th and REEs were analyzed by ICP-MS at Activation Laboratories.

Isotope Geochemistry

Preparation and analysis of samples for isotope geochemistry took place in three laboratories. All Sr and Pb samples were prepared and analyzed at the Isotope

TABLE 1

Representative mineral compositions from rocks of the Lincoln syenite

	Potassium-Feldspar				Plagioclase		
	MR-30 Core	MR-30 Rim	MR-30 Matrix	SLR-11 Matrix	MR-1 Plag3	MR-30 Albite	SLC-10 Plag1
SiO_2	64.59	64.97	64.96	64.71	63.51	68.82	61.26
Al_2O_3	19.04	18.34	18.66	18.22	23.20	19.65	24.84
FeO	0.17	0.00	0.06	0.12	0.06	0.12	0.01
MnO	0.00	0.10	0.00	0.00	0.00	0.00	0.01
MgO	0.00	0.00	0.02	0.00	0.00	0.01	0.00
CaO	0.25	0.01	0.08	0.00	4.77	0.36	6.65
BaO	1.12	0.38	0.39	0.09	0.00	0.00	0.00
K_2O	11.66	14.88	13.19	15.44	0.25	0.08	0.09
Na_2O	3.06	0.92	2.24	0.78	8.57	11.10	7.72
Total	**99.89**	**99.60**	**99.60**	**99.36**	**100.36**	**100.14**	**100.58**
Formula per 8 O							
Si	2.969	3.004	2.990	3.004	2.797	2.997	2.706
Al	1.031	1.000	1.012	0.997	1.204	1.009	1.293
Fe	0.006	0.000	0.002	0.005	0.002	0.004	0.000
Mn	0.000	0.004	0.000	-0.001	0.000	0.000	0.000
Mg	0.000	0.000	0.001	0.000	0.000	0.001	0.000
Ca	0.012	0.000	0.004	0.000	0.225	0.017	0.315
Ba	0.020	0.007	0.007	0.002	0.000	0.000	0.000
K	0.685	0.878	0.775	0.914	0.014	0.004	0.005
Na	0.272	0.083	0.199	0.070	0.732	0.937	0.661
Total	**4.995**	**4.976**	**4.990**	**4.991**	**4.974**	**4.969**	**4.981**

Geochemistry Laboratory, Department of Geology, University of Maryland. Preparation of Nd samples took place in the Department of Earth Sciences at SUNY-Oswego with separation of Nd from REE concentrates performed at the Radiogenic Isotope Laboratory of the Geology Department at Syracuse University. A portion of the Nd isotope analyses were made at Maryland and the remainder were analyzed at Syracuse. Summary details of these procedures follow.

Samples for Sr isotope analysis were digested overnight in screw-top Teflon® vials in a mixture of concentrated HF and HNO_3, evaporated and attacked with concentrated HCl, evaporated again, and dissolved in 2 M HCl. Isolation of Sr used columns with 2 ml AG 50W-x8 cation exchange resin followed by columns with c. 0.15 ml Sr-specific resin (Eichrom Technologies, Inc.). The procedural blank during this study ranged from 0.39 to 0.61 ng ($^{87}Sr/^{86}Sr \sim 0.729$) and > 1 μg of sample Sr was processed for all samples.

As indicated previously, alkali feldspar crystals from the Lincoln syenite contain ubiquitous mineral inclusions of various sizes. Even with fine crushing, the isolation of verifiably inclusion-free grains was impractical. Crystals were crushed to pass a 120 μm sieve and the lowest density fraction from flotation in "LST" liquid was sequentially passed through a Frantz magnetic separator to deliver a least inclusion rich fraction of

TABLE 1
(continued)

Ilmenite			Magnetite		Biotite		
	MR-25	SLC-11	MR-25			MR-25	SLC-11
	Ilm2	Ilm1	Mag1	Mag2	SiO_2	38.62	39.09
TiO_2	47.74	43.84	0.55	0.44	TiO_2	5.19	4.61
Nb_2O_5	0.35	0.30	0.04	0.00	Al_2O_3	12.74	12.48
Ta_2O_5	0.01	0.00	0.00	0.00	Cr_2O_3	0.22	0.10
Al_2O_3	0.02	0.00	0.05	0.51	FeO	11.97	11.61
V_2O_3	0.56	0.56	0.73	1.32	MnO	0.03	0.04
Cr_2O_3	0.23	0.24	1.64	11.78	MgO	16.69	17.20
Fe_2O_3 [calc]	8.28	14.77	65.43	54.23	CaO	0.03	0.00
FeO	41.34	38.43	31.52	30.75	BaO	0.18	0.01
MnO	0.70	0.81	0.00	0.07	K_2O	9.61	9.74
ZnO	0.00	0.06	0.03	0.22	Na2O	0.13	0.09
MgO	0.71	0.24	0.00	0.12	F	0.78	0.85
SnO	0.01	0.04	0.00	0.04	Cl	0.10	0.13
WO_3	0.00	-0.01	0.00	0.00	H_2O [calc]	3.67	3.63
Total	99.95	99.28	99.99	99.48	Total	99.94	99.58
					F,Cl=O	.35	.39
					Total	99.59	99.19
Formula per 2 cat. and 3 O			Formula per 3 cat. and 4 O		Formula per 24 O		
Ti	0.908	0.845	0.016	0.013	Si	5.699	5.773
Nb	0.004	0.003	0.001	0.000	Al	2.215	2.172
Ta	0.000	0.000	0.000	0.000	Total	7.914	7.945
Al	0.001	0.000	0.002	0.023			
V	0.009	0.009	0.019	0.034	Al	0.000	0.000
Cr	0.005	0.005	0.050	0.358	Ti	0.576	0.512
Fe^{+3} [calc]	0.157	0.286	1.895	1.570	Cr	0.025	0.011
Fe^{+2}	0.874	0.824	1.016	0.989	Fe	1.477	1.434
Mn	0.015	0.018	0.000	0.002	Mn	0.004	0.005
Zn	0.000	0.001	0.001	0.006	Mg	3.671	3.786
Mg	0.027	0.009	0.000	0.007	Total	5.753	5.748
Sn	0.000	0.000	0.000	0.001			
W	0.000	0.000	0.000	0.000	Ca	0.005	0.000
Total	2.000	2.000	3.000	3.000	K	1.809	1.835
					Na	0.037	0.026
					Total	1.851	1.861
					F	0.364	0.395
					Cl	0.025	0.033
					H [calc]	3.611	3.572
					Total	4.000	4.000
					Total	19.518	19.554

TABLE 1
(continued)

	Pyroxene				SLC-10 Olivine	
	SLC-10 Opx-core	SLC-10 Opx-rim	MR-30 Cpx-core	MR-30 Cpx-rim	Olivine-1	Olivine-3
SiO_2	54.61	53.44	52.14	52.58	37.31	37.25
TiO_2	0.02	0.14	0.76	0.41		
Al_2O_3	0.30	1.04	1.19	0.93		
Cr_2O_3	0.00	0.05	0.30	0.10		
FeO^T	16.85	19.71	8.30	8.44		
$Fe_2O_3^{[calc]}$	1.01	0.61	1.80	2.01		
FeO	15.94	19.16	6.68	6.63		
MnO	0.25	0.32	0.21	0.24		
MgO	27.28	24.43	15.15	14.75		
CaO	0.45	0.78	20.52	20.96		
K_2O	0.00	0.01	0.01	0.00		
Na_2O	0.00	0.00	0.60	0.69		
Total	**99.86**	**99.98**	**99.36**	**99.30**		
	Formula per 4 cations and 6 O					
Si	1.979	1.965	1.945	1.963		
Al	0.013	0.035	0.052	0.037		
Fe^{+3}(iv)	0.008	0.000	0.003	0.000		
Total	**2.000**	**2.000**	**2.000**	**2.000**		
Al(vi)	0.000	0.010	0.000	0.004		
Ti	0.001	0.004	0.021	0.012		
Fe^{+3}(vi)	0.017	0.016	0.047	0.056		
Fe	0.483	0.588	0.209	0.207		
Cr	0.000	0.001	0.009	0.003		
Mn	0.008	0.010	0.007	0.008		
Mg	1.474	1.339	0.843	0.821		
Ca	0.017	0.031	0.820	0.839		
K	0.000	0.001	0.000	0.000		
Na	0.000	0.000	0.044	0.050		
Total	**2.000**	**1.991**	**2.000**	**2.000**		
Total	**4.000**	**4.000**	**4.000**	**4.000**		
					Formula per 4 O	
					Si	0.994	0.997
					P	0.001	0.002
					Al	0.000	0.001
					Cr	0.000	0.000
					Fe	0.613	0.646
					Mn	0.007	0.006
					Ni	0.004	0.005
					Mg	1.386	1.345
					Ca	0.000	0.000
					K	0.000	0.000
					Na	0.000	0.000
					Total	**3.005**	**3.002**

10 to 20 mg. These grains were soaked in closed Teflon® vials containing 1 to 2 ml of 50:50 6 M HCL and 7 M HNO_3 at 100°C for at least 48 hours. The resultant grains were rinsed three times with water and attacked with HF until approximately 75 percent of the original volume (by visual estimation) had been destroyed. The intention was to eradicate biotite and pyroxene inclusions during the cleaning and leaching. Inclusions of rutile should resist such attacks as well as the subsequent digestion, and thus not contribute Pb to the final solution that goes through ion exchange. The remaining

solid was digested, evaporated and taken up in 0.6 M HBr, and Pb was separated using columns with c. 0.12 ml AG1-x8 anion exchange resin. The total Pb blank was 130 to 370 pg, of which 1 to 4 pg was introduced during loading.

Samples for Nd isotope analysis were prepared by flux fusion, Fe-co-precipitation, and bulk REE separation by cation exchange, following Tomascak and others (1996). Neodymium was subsequently separated from the REE concentrates using dilute HCl and Teflon powder equilibrated with HDEHP (Samson and others, 1995). In excess of 10 μg Nd was processed for each sample.

Strontium and Pb isotope ratio measurements were carried out using a VG Sector 54 mass spectrometer with seven in-line faraday cups. Measured Sr isotope ratios normalized to $^{86}Sr/^{88}Sr = 0.1194$. Analyses of NIST standard SRM-987 (100 ng on Re filaments, with Ta_2O_5) during the study yielded a mean $^{87}Sr/^{86}Sr$ of 0.710248±18 (2σ; n = 30).

A fractionation correction of 0.079 ± 0.008% amu^{-1} was applied to the Pb isotope data, referenced relative to the updated recommended isotopic values of NBS Pb standard SRM-981 (Thirlwall, 2000). The Pb standard analyses made throughout the study yielded a mean reproducibility of ± 0.032% amu^{-1} (2σ; n = 16) for ratios involving measurement of ^{204}Pb, which was similar to the reproducibility for replicate measurements of individual samples.

Neodymium isotope ratio measurements were carried out at Maryland and Syracuse, although essentially identical mass spectrometers and consistent analytical methods were used. Measured Nd isotope ratios were normalized to $^{146}Nd/^{144}Nd = 0.72190$ in all cases. At Maryland, analyses of the La Jolla Nd standard during the study yielded a mean $^{143}Nd/^{144}Nd$ of 0.511844 ± 16 (2σ; n = 10). A value of 0.511849 ± 12 was measured in the Syracuse laboratory. Considering both reproducibility of $^{143}Nd/^{144}Nd$ and imprecision of the ratio Sm/Nd (from comparison of ICP-MS and previous isotope dilution measurements), uncertainty on $\varepsilon_{Nd(t)}$ is ± 0.4 unit.

RESULTS

Mineral Compositions

The chemistry of the major phases present the Lincoln syenite is discussed below and representative mineral compositional data are reported in table 1. Figure 5 provides an overview of typical compositional zoning within the large alkali feldspar megacrysts and pyroxene rim compositions are portrayed graphically in figure 6.

Alkali feldspar.—Alkali feldspar in the Lincoln syenite occurs both as large macroscopically zoned euhedral to subhedral megacrysts (fig. 3) and as finer grained anhedral constituents of the groundmass. The megacrysts show non-coincident oscillatory zoning in both Ba and Na/K (fig. 5). Higher Ba concentrations (up to 1.6 wt. %) along with more sodic compositions typically occur in the cores of the megacrysts suggesting a higher temperature of crystallization (Long and Luth, 1986). Albite exsolution is commonly observed at the microscopic scale with lower potassium zones containing greater concentrations of albite lamellae. The fine intergrowth of lamellae precluded reliable separate analysis of either phase in many locations, but rolling averages along linear traverses show the high temperature composition range from about $Or_{55}Ab_{45}$ to $Or_{90}Ab_{10}$. The chemistry of the megacryst outer margins (low in Ba and relatively high in K) are indistinguishable from the chemistry of the matrix alkali feldspar (see fig. 5) and suggest the growth of the megacryst rims coincided with the growth of groundmass alkali feldspar.

Plagioclase feldspar.—While microscopic albite lamellae are common within the large alkali feldspar megacrysts, plagioclase feldspar is not a modally abundant primary crystallizing phase in rocks of the Lincoln syenite. When present, it is found as

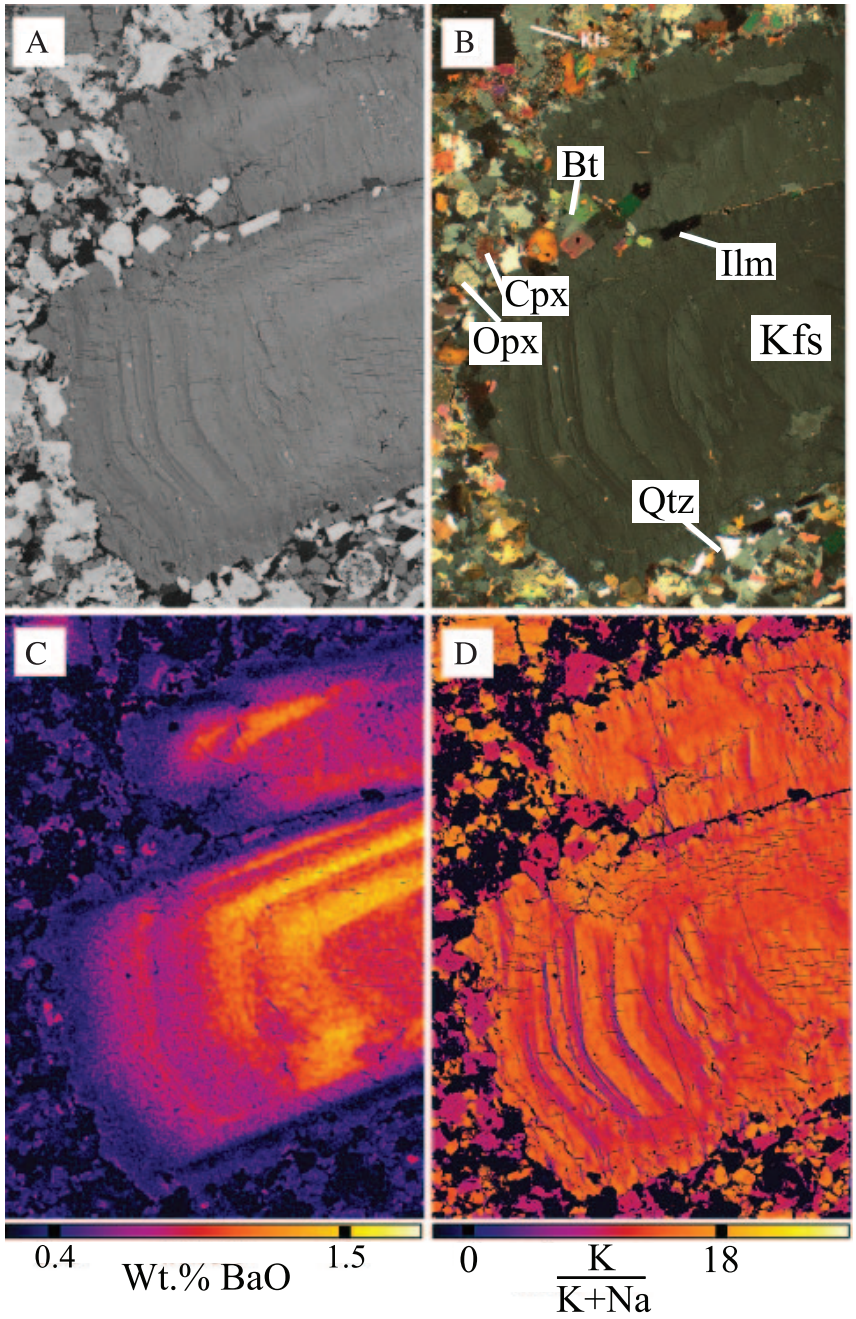

Fig. 5. Zoned potassium feldspar megacryst (1.38cm across). (A) backscattered electron stage scan map, (B) photomicrograph, crossed polarized light; (C) Ba Lα x-ray stage scan map, (D) K Kα x-ray stage scan map. Kfs - potassium feldspar, Qtz – quartz, Cpx – augite, Opx – enstatite, Ilm – ilmentite, Bt – biotite.

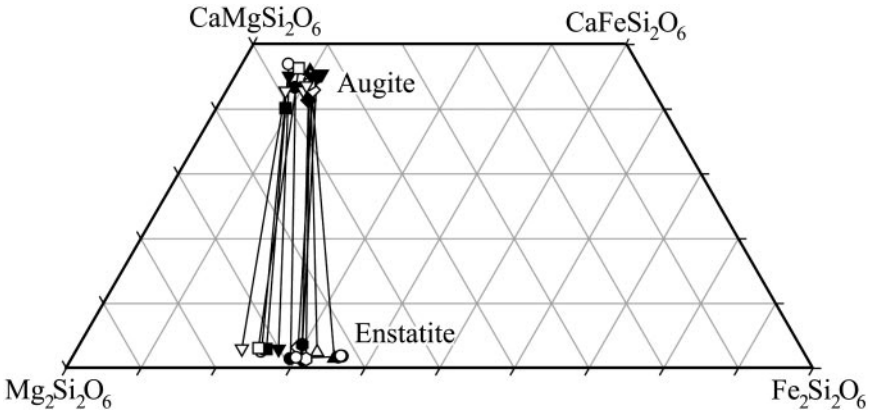

Fig. 6. Pyroxene quadralateral showing coexisting clinopyroxene – orthopyroxene rim compositions. Solid lines connect adjacent clinopyroxene – orthopyroxene grains (shown with similar symbols).

anhedral to subhedral grains in the groundmass with a composition ranging from approximately An_{25} to An_{35}, and is commonly rimmed or contains rounded inclusions of albite.

Pyroxenes.—Both ortho- and clinopyroxene are modally abundant in samples that have not been affected by post-crystallization processes. Orthopyroxene is euhedral to subhedral, weakly pleochroic, and up to 2.0 mm across. The orthopyroxenes (enstatite) are relatively Mg-rich with average compositions being approximately $En_{70}Fs_{27}Wo_3$. Most grains are zoned with respect to Mg/Fe with cores being more Mg-rich. Clinopyroxene is generally subhedral to anhedral, inclusion rich, and up to 3.5 mm across. Similar to the orthopyroxenes, the clinopyroxene (augite) is quite Mg-rich plotting close to $CaMgSi_2O_6$ in composition (fig. 6). Augite cores are slightly more enriched in Mg relative to the rims. Most augite grains analyzed contain significant amounts of non-quadrilateral components (for example, Fe_2O_3, Al_2O_3, TiO_2).

Biotite.—Biotite is a common and modally abundant phase in all rocks of the Lincoln syenite. It is generally subhedral, typically up to 6.0 mm across, although in some orthopyroxene rich rocks close to the northwestern margin, biotite is observed to be up to 15.0 mm across. Chemically, the biotite is Mg-rich ($Mg/(Mg+Fe) \sim 0.7$), very rich in TiO_2 (~ 5 wt %), contains measurable amounts of Cr_2O_3 and fluorine.

Olivine.—Olivine has only been found in the relatively fine-grained, non-porphyritic border phase of the Lincoln syenite and in these rocks it is scarce ($< 1\%$). It occurs as isolated grains up to 3.0 mm across that are completely mantled by orthopyroxene (fig. 4C). Compositionally the olivine is approximately Fo_{70} and shows little compositional variability.

Oxide minerals.—In thin section, oxide minerals are generally subhedral to anhedral and up to 0.7 mm across. Electron microprobe analysis of the oxide minerals reveal significant complexity. Ilmenite contains visible fine-scale hematite exsolution lamellae and "ilmenite" probe analyses are likely a composite of ilmenite and hematite. These analyses show measurable Cr, V, and Nb. Magnetite is also present in all samples analyzed and it is commonly intergrown with ilmenite. This magnetite commonly contains large amounts of Cr_2O_3.

Whole Rock Geochemistry

The whole rock major and trace element chemistry for rocks of the Lincoln syenite presented in table 2 indicates all the rocks are intermediate in composition

TABLE 2

Major and trace element contents of the Lincoln syenites

Sample	***SLC-10****	***SLC-11***	***1018***	***MR-1***	***MR-2C****	***MR-8***	***MR-10***	***MR-11***
Latitude	*44.3212*	*44.3216*	*44.3530*	*44.3184*	*44.3158*	*44.3215*	*44.3261*	*44.3259*
Longitude	*69.3591*	*69.3587*	*69.2833*	*69.3574*	*69.3519*	*69.3588*	*69.3489*	*69.3396*
SiO_2	59.08	57.35	57.62	59.12	54.01	58.12	57.49	56.60
TiO_2	1.28	1.26	1.27	1.46	1.45	1.26	1.33	1.33
Al_2O_3	11.91	11.85	12.21	11.25	8.76	11.65	11.77	10.71
Fe_2O_3(t)	6.14	6.73	6.52	6.56	9.36	6.52	6.21	7.34
MnO	0.09	0.09	0.09	0.09	0.15	0.09	0.09	0.11
MgO	7.24	7.67	6.99	7.47	11.90	7.58	7.26	8.74
CaO	4.24	4.40	4.15	4.72	6.50	4.34	4.05	4.65
Na_2O	1.55	2.31	2.30	1.91	1.31	2.22	2.27	1.96
K_2O	7.17	6.80	7.03	6.14	5.20	6.71	6.94	6.29
P_2O_5	0.66	0.75	0.73	0.78	1.12	0.77	0.73	0.87
Total	99.36	99.21	98.91	99.50	99.76	99.26	98.14	98.60
Sc	16	16	16	19	24	17	16	18
V	165	169	170	174	224	174	170	194
Cr	465	498	430	424	724	489	479	580
Co	28	31	28	22	50	36	35	38
Ni	189	193	156	131	281	227	214	212
Cu	67	78	49	72	92	124	105	73
Zn	119	79	68	30	83	102	120	64
Rb	300	384	409	278	378	407	444	376
Sr	555	570	503	775	334	607	694	628
Y	27.0	28.0	28.0	38.4	42.6	26.9	27.8	31.5
Zr	674	730	849	683	368	675	1120	793
Nb	38.5	54.5	57.0	25.8	38.7	40.5	46.5	37.0
Ba	1510	1530	1587	1770	736	1467	1772	1610
La	73.0	93.0	95.2	66.7	96.3	80.4	79.2	77.8
Ce	145	179	180	146	210	174	172	167
Pr	18.0	20.8	20.6	16.6	27.7	20.6	20.2	21.4
Nd	67.0	76.2	80.0	62.3	100.0	81.5	79.4	76.7
Sm	14.0	15.5	16.1	15.0	23.4	15.6	15.4	14.9
Eu	2.80	2.78	3.00	2.75	3.78	2.92	2.89	2.88
Gd	10.70	11.41	11.10	9.31	12.90	9.80	9.76	11.2
Tb	1.20	1.20	1.60	1.33	1.76	1.22	1.22	1.30
Dy	5.96	6.04	6.02	7.57	8.99	5.78	5.82	5.86
Ho	1.08	1.09	1.07	1.32	1.41	0.99	0.99	1.03
Er	2.79	2.69	2.71	3.17	3.47	2.71	2.82	3.01
Tm	0.43	0.40	0.42	0.43	0.49	0.37	0.41	0.38
Yb	2.50	2.55	2.63	3.10	3.41	2.25	2.49	2.30
Lu	0.38	0.38	0.39	0.47	0.48	0.36	0.39	0.38
Hf	15.6	19.7	20.5	16.6	11.2	18.8	29.9	20.6
Ta	2.30	3.00	3.10	2.45	3.30	3.00	3.30	3.05
Th	40.1	66.6	73.8	39.3	44.0	58.1	54.1	71.5
U	7.0	19.0	17.0	15.1	7.58	18.0	21.3	13.8

Major elements are in wt % oxide and trace elements in ppm. Majors and Sc, V, Cr, Co, Ni, Cu and Zn analyzed by ICP-OES at Middlebury College. Other trace elements analyzed by ICP-MS at Activation Labs in Ancaster, Ontario. * = Chilled margin sample; ** = Mafic enclave sample

TABLE 2
(continued)

Sample	***MR-13***	**MR-15a**	***MR-20***	***MR-23***	***MR-25***	***MR-30***	***MR-44***	***MR-50***	***MR-51***
Latitude	*44.3151*	*44.3111*	*44.3656*	*44.3136*	*44.3155*	*44.3007*	*43.8486*	*44.3214*	*44.3211*
Longitude	*69.3361*	*69.3494*	*69.2786*	*69.3517*	*69.3549*	*69.3241*	*69.6504*	*69.3511*	*69.3493*
SiO_2	56.23	55.19	55.29	56.54	56.26	55.53	55.98	56.52	57.04
TiO_2	1.44	1.41	1.35	1.40	1.39	1.57	1.37	1.45	1.35
Al_2O_3	11.58	10.82	10.67	11.00	10.77	11.40	10.68	10.85	11.62
Fe_2O_3(t)	7.07	7.38	7.34	7.67	7.94	7.48	7.52	7.51	6.58
MnO	0.10	0.11	0.10	0.11	0.12	0.11	0.12	0.11	0.10
MgO	7.96	8.89	9.12	8.99	9.49	8.19	8.93	8.25	7.86
CaO	4.45	5.41	4.97	4.92	5.32	4.78	5.04	4.53	4.10
Na_2O	2.00	1.89	1.53	1.97	1.94	2.04	1.89	1.92	2.13
K_2O	6.98	6.37	6.62	6.38	6.20	6.61	6.39	6.55	6.68
P_2O_5	0.85	0.92	0.90	0.93	0.97	0.90	0.93	0.92	0.78
Total	98.66	98.39	97.89	99.91	100.40	98.61	98.85	98.61	98.24
Sc	17	21	19	19	19	18	20	19	16
V	191	191	180	207	194	223	209	207	173
Cr	499	406	549	591	579	493	554	532	476
Co	38	29	39	43	38	36	38	36	36
Ni	220	180	228	243	236	215	246	207	209
Cu	109	76	60	104	120	92	101	100	93
Zn	115	74	111	93	97	93	88	84	109
Rb	398	330	356	362	326	345	343	321	351
Sr	694	596	585	750	761	676	890	735	566
Y	28.6	27.7	27.9	33.8	35.1	34.2	34.1	35.1	27.0
Zr	699	564	631	434	643	1170	503	1010	545
Nb	43.9	45.6	31.9	41.0	39.2	37.4	32.4	37.3	37.1
Ba	1851	1777	1660	2100	2040	1730	2410	1820	1510
La	79.1	89.4	74.6	81.9	94.3	81.3	88.5	89.4	71.7
Ce	171	193	170	176	189	183	178	191	162
Pr	20.5	23.6	20.7	22.3	21.8	22.1	21.9	21.2	19.4
Nd	83.5	93.6	85.6	82.3	86.4	76.9	88.4	78.8	78.4
Sm	16.2	18.2	16.8	16.3	19.4	16.2	18.2	18.1	15.3
Eu	3.05	3.38	3.18	3.11	3.40	3.33	3.35	3.45	2.89
Gd	10.2	12.4	10.9	11.8	10.6	11.5	11.4	10.4	9.97
Tb	1.27	1.46	1.36	1.37	1.46	1.26	1.50	1.28	1.23
Dy	5.82	6.67	6.06	6.30	7.44	6.29	7.04	7.05	5.72
Ho	1.02	1.10	1.00	1.11	1.16	1.17	1.12	1.16	0.96
Er	2.80	3.00	2.77	3.09	2.87	3.03	3.01	2.84	2.59
Tm	0.37	0.42	0.36	0.38	0.40	0.36	0.41	0.37	0.36
Yb	2.27	2.61	2.25	2.38	2.84	2.47	2.61	2.79	2.25
Lu	0.35	0.39	0.34	0.38	0.40	0.42	0.37	0.43	0.34
Hf	17.8	16.7	16.7	12.3	17.3	25.0	13.7	22.2	14.6
Ta	2.56	2.64	1.85	3.00	3.15	2.29	2.14	2.63	2.07
Th	30.3	68.8	25.0	42.4	51.0	27.2	28.0	32.6	22.6
U	10.40	18.22	7.03	12.50	13.00	6.71	7.34	8.10	6.08

(SiO_2 = 55 to 60 wt %). The rocks are characterized by very high concentrations of K_2O (5 – 7 wt%), Ba (up to 2400 ppm) and Rb (up to 450 ppm) along with high contents of MgO (6 – 9 wt.%), Ni (100 – 250 ppm) and Cr (400 – 600 ppm). The rocks

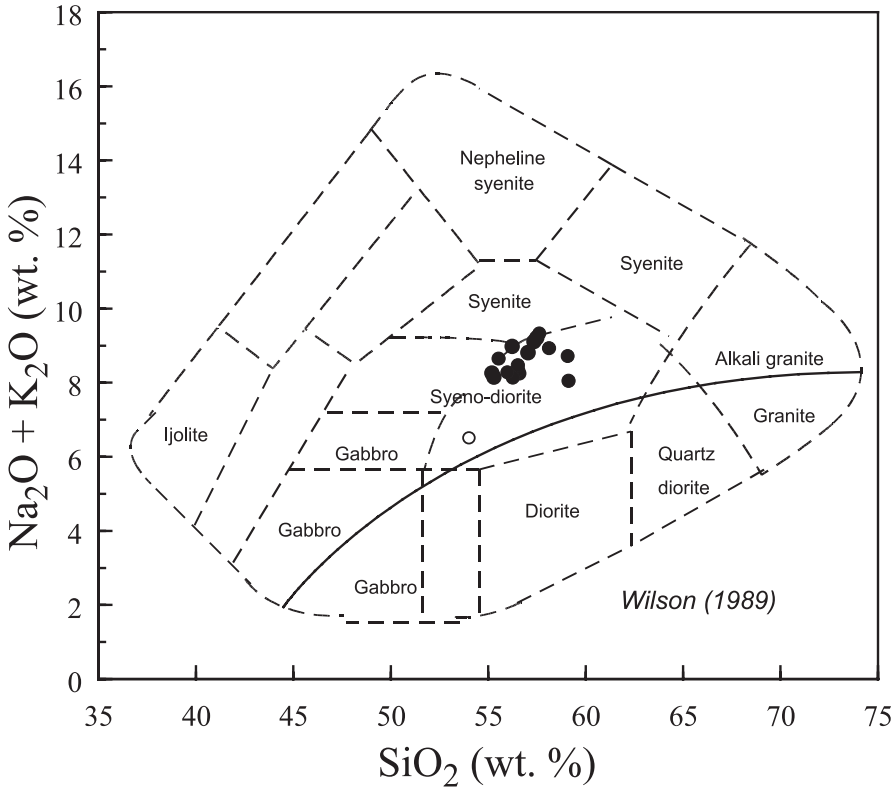

Fig. 7. Chemical classification of rocks of the Lincoln syenite using a total alkali-silica diagram (Wilson, 1989). These rocks would fall into the trachyandesite field on a similar diagram for volcanic rocks (Le Bas and others, 1986). The open circle in this and all other diagrams represents the mafic enclave sample

are classified chemically as an alkaline syeno-diorite (or trachyandesite in volcanic rock terminology) in a total alkalis versus silica diagram (fig. 7). It should be noted that the high alkaline content is due to the unusually high concentration of K_2O in the rocks and not the Na_2O content, which is in the "normal" range for intermediate rocks. All samples analyzed, including the mafic enclave and chilled margin samples, meet the definition for ultrapotassic rocks as provided by Foley and others (1987), that is they have $MgO > 3\%$, $K_2O > 3\%$, and $K_2O/Na_2O > 2.0$.

Despite sampling the range of rock types observed within the syenite body, for the most part, there is surprisingly little major and trace element variability among the 20 analyzed samples (table 2 and figs. 7, 8, and 9). Harker diagrams show that as the silica content increases from 55 to 60 weight percent, MgO, CaO, TiO_2, Cr and Ni decrease slightly whereas Al_2O_3, Na_2O and K_2O remain fairly constant. Ba, Rb, Zr, and Sr show larger variability with no systematic trends with respect to SiO_2 content.

Rare earth element (REE) patterns are similar for all samples and cluster tightly (fig. 10). The samples are more enriched in the light rare earth elements (LREE) at 100 to 200X chondrite than the heavy rare earth elements at 10X chondrite; thus, the overall patterns have a negative slope that flatten in the region from Dy to Lu on the diagram. Ratios of $(La/Sm)_N$ range from 2.5 to 3.7, $(La/Yb)_N$ from ~14 to ~25 and $(Sm/Yb)_N$ from ~ 5 to 8. A small negative Eu anomaly occurs in all samples.

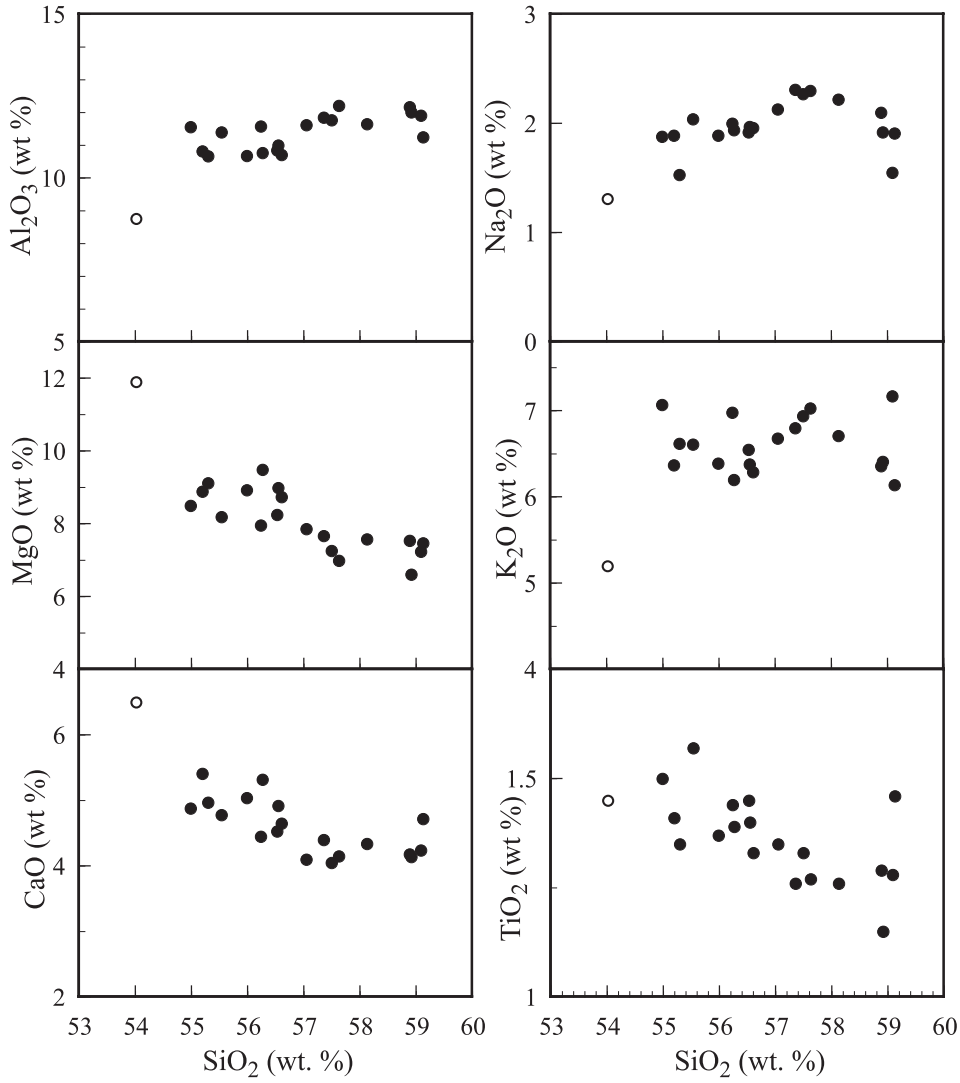

Fig. 8. Harker variation diagrams for major elements in rocks of the Lincoln syenite.

Extended rare earth diagrams show that all Lincoln syenite samples are strongly enriched in more incompatible elements relative to less incompatible elements (fig. 11). In particular, Rb, Ba, Th, U and K are enriched relative to all other elements. Distinct negative anomalies are seen for Nb (relative to U and K), Sr (relative to Pr and P), Ti (relative to Eu and Dy), and Ba (relative to Rb and Th). In both rare earth and extended rare earth diagrams, samples do differ in absolute abundance of the elements by small percentages, but the patterns generally are parallel to one another with few crossing patterns seen. A notable exception to this is seen in Zr content, which shows much more variability than other elements, perhaps due to inhomogeneous distribution of zircon grains in the rock. Ba also shows more variation than is apparent

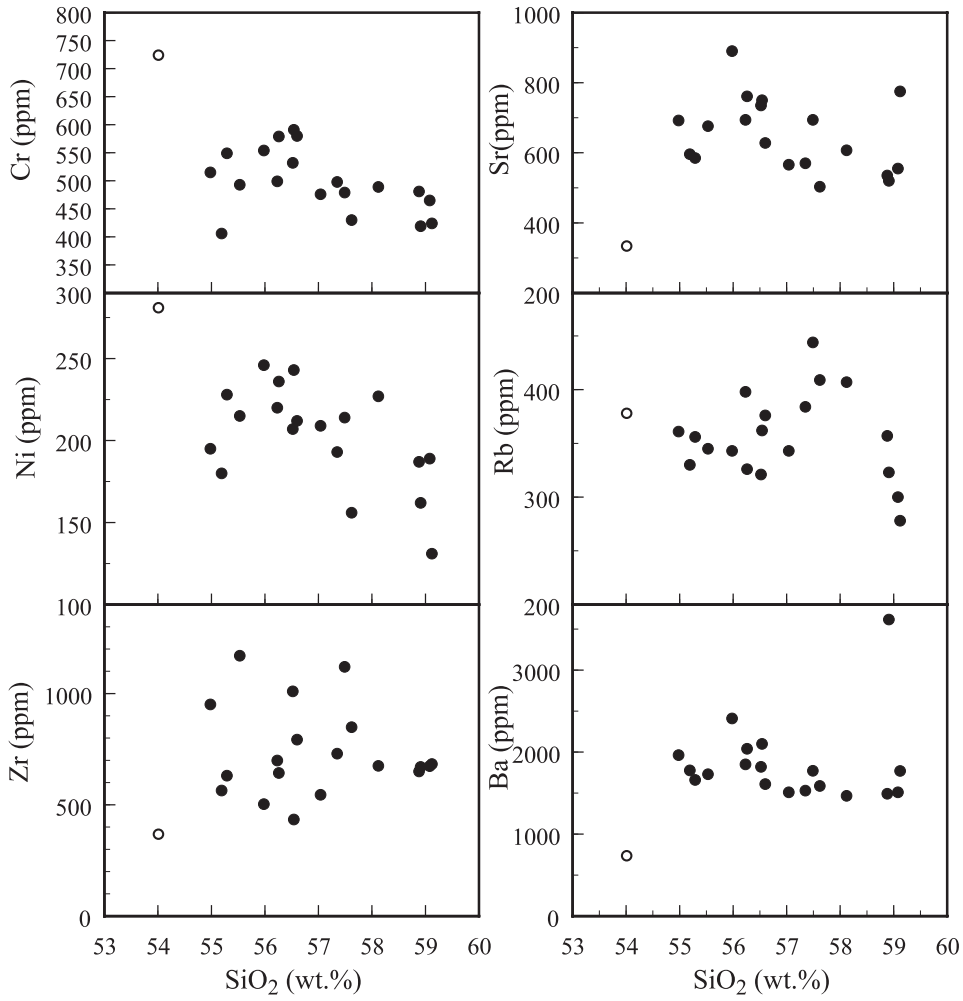

Fig. 9. Harker variation diagrams for trace elements in rocks of the Lincoln syenite.

for most other elements, although the negative Ba anomaly in the extended rare earth diagram is still preserved in all samples.

The overall variability of major and trace element abundances (figs. 7, 8, and 9) is in some cases (for example, K_2O, Ba) likely due to differences in the modal abundance of the alkali feldspar megacrysts present in individual samples. However, it should be pointed out that both the chilled margin and mafic enclave samples lack alkali feldspar megacrysts and yet they still preserve the distinctive geochemical signatures of the alkali feldspar megacryst-bearing rocks. In particular, the rare earth element patterns (figs. 10 and 11) of the mafic enclave and chilled margin samples are indistinguishable from those of the alkali feldspar megacryst-bearing samples.

Isotope Geochemistry

The whole rock isotopic compositions of strontium and neodymium, along with alkali feldspar lead isotopic compositions are presented in table 3. Although samples

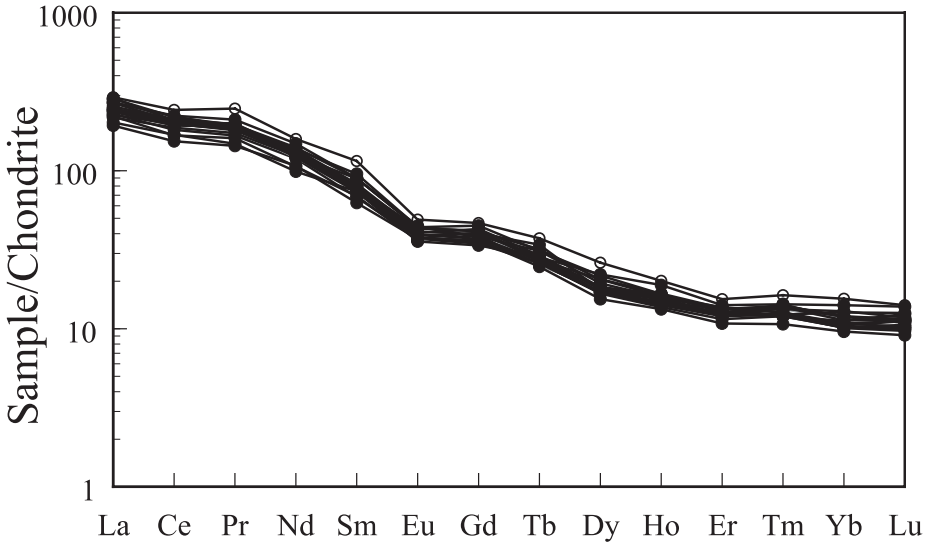

Fig. 10. Chondrite-normalized (Nakamura, 1974) plot for rocks of the Lincoln syenite.

are monotonous in terms of Rb content, the enclave has significantly lower Sr, and hence Rb/Sr that is > 2x that of the syenites proper. In terms of Sr isotopes, this translates to a somewhat lower calculated initial $^{87}Sr/^{86}Sr$. Nonetheless, all samples, including the mafic enclave, have initial Sr ratios that are higher than modern pristine mantle rocks (range from 0.7069 – 0.7105). The samples, excluding the enclave MR-2c, fall about a 418 Ma reference line. Their lack of variation in Rb/Sr precludes

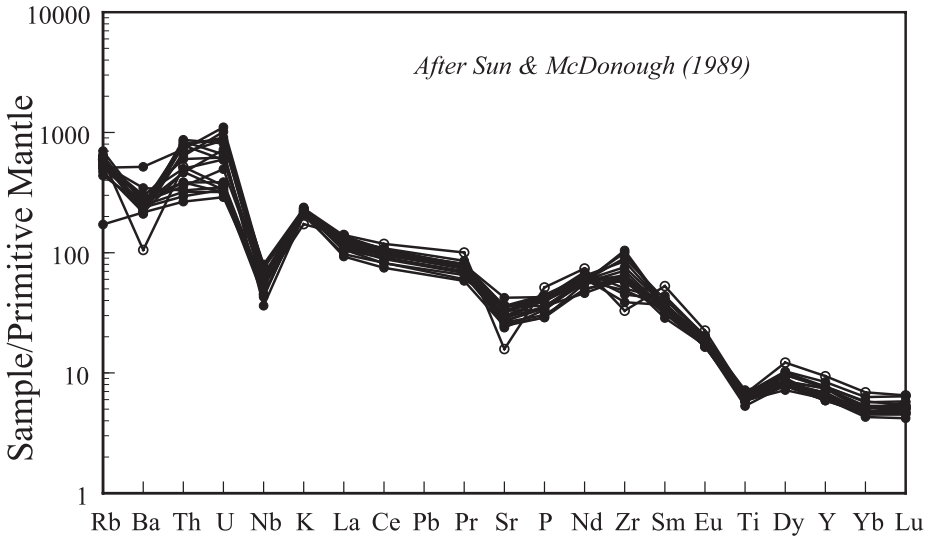

Fig. 11. Primitive mantle-normalized (Sun and McDonough, 1989) extended element diagram for rocks of the Lincoln syenite.

TABLE 3

Isotope data for Lincoln syenite samples

	$^{87}Rb/^{86}Sr$	$^{87}Sr/^{86}Sr$ [a]	$^{87}Sr/^{86}Sr$ @ 418 Ma	$^{147}Sm/^{144}Nd$	$^{143}Nd/^{144}Nd$ [a]	$\varepsilon_{Nd\ (418Ma)}$	$^{206}Pb/^{204}Pb$ [b]	$^{207}Pb/^{204}Pb$ [b]	$^{208}Pb/^{204}Pb$ [b]
MR-1	1.04	0.716713 (16)	0.7105	0.1456	0.512157 (11) [c]	-6.7	18.308 (1)	15.614 (1)	38.078 (3)
MR-11	1.74	0.720539 (8)	0.7102	---	---	---	18.332 (2)	15.639 (2)	38.155 (4)
MR-23	1.40	0.716722 (12)	0.7084	0.1197	0.512178 (8)	-4.9	18.318 (2)	15.629 (2)	38.122 (6)
MR-25	1.24	0.716530 (20)	0.7091	0.1357	0.512205 (7) [c]	-5.2	18.308 (4)	15.612 (4)	38.073 (8)
MR-30	---	---	---	---	---	---	18.304 (1)	15.613 (1)	38.069 (3)
MR-44	1.12	0.715631 (16)	0.7090	0.1245	0.512187 (7) [c]	-5.0	18.337 (1)	15.603 (1)	38.051 (3)
MR-50	1.27	0.716387 (10)	0.7089	0.1389	0.512191 (7) [c]	-5.6	18.280 (2)	15.577 (1)	37.957 (4)
SLC-10	1.57	0.717789 (9)	0.7085	0.1230	0.512175 (8)	-5.3	---	---	---
SLC-11	1.95	0.720155 (9)	0.7085	0.1263	0.512192 (9) [c]	-4.8	---	---	---
MR-2c	3.28	0.726438 (9)	0.7069	0.1415	0.512195 (8)	-5.7	---	---	---

note: — = not determined; parent/daughter ratios use concentrations from table 2

[a]measured values, corrected for blank and fractionation; absolute 2σ within-run uncertainty on last digit(s) of individual analysis in parentheses

[b]measured value of leached feldspar residue, corrected for fractionation; absolute 2σ within-run uncertainty on last digit(s) of individual analysis in parentheses

[c]Nd analyzed at Syracuse University (see text)

geochronometry by this system. Linear regression of all nine samples together gives an apparent age of 340 ± 68 Ma, controlled in large part by the high Rb/Sr enclave sample

With the exception of sample MR-1, the initial Nd isotopic compositions of all samples including enclave MR-2c show only 0.09 permil variability, with initial (418 Ma) ε_{Nd} values ranging from -4.8 to -5.7 (table 3). The Sm/Nd ratios of the samples are rather variable, although all are subchondritic. Despite the homogeneity of initial ratios, samples do not show meaningful geochronological relations. The initial ratios are lower, mostly significantly so, than granitic rocks and their metasedimentary hosts from southern and southwestern Maine (Tomascak and others, 1996, 1999).

The alkali feldspar separates from the Lincoln syenite samples show limited Pb isotope variability. The ratios of are typical of igneous rocks from central Maine, as defined by Ayuso and Bevier (1991) (fig. 12). The budget of Pb in alkali feldspar is sufficiently high that, even if the procedure to screen out very inclusion-rich grains proved ineffective, Pb should still be dominated by the common component. Although rutile may be expected to have much higher U/Pb than feldspars, Pb concentrations are low and variable (Mezger and others, 1989). Considering this, and given the nature of the chemical treatment of samples, rutile inclusions are not expected to contribute meaningfully to the measured Pb isotope ratios.

PETROGENESIS OF THE LINCOLN SYENITE

Any petrogenetic model for the Lincoln syenite must account for the following geochemical characteristics: (1) Despite intermediate SiO_2 compositions (55 – 59%), the rocks are primitive in terms of their MgO (Mg# > 67), Cr (> 400 ppm), and Ni (> 150 ppm) contents (fig. 13). (2) The rocks are characterized by extreme enrichments in the large ion lithophile elements (for example, 6 - 7 wt.% K_2O, and 1500 - 2400 ppm Ba) along with high concentrations of light rare earth elements (200 – 300x chondrite abundances). (3) The syenites are relatively depleted in the high field strength elements (for example, Nb, Ta). (4) The rocks show limited radiogenic isotopic variability with relatively high initial $^{87}Sr/^{86}Sr$ values (0.707 to 0.710), relatively low initial ε_{Nd} values (-4.8 to -6.7) and initial $^{207}Pb/^{204}Pb$ values are relatively high (> 15.57).

Source of the Ultrapotassic Magma

Relatively mafic (that is, Mg# > 65) yet ultrapotassic ($K_2O/Na_2O > 2.0$) igneous rocks similar to those of the Lincoln syenite, while restricted in geological occurrence, have received considerable petrologic interest (Foley, 1992a). The origin of the potassium, along with the abundance of other what are generally thought to be crustally derived large ion lithophile elements (for example, Ba, Rb, Sr) in combination with relatively high abundances of mantle derived primitive elements (for example, Mg, Ni, Cr) requires a unique petrologic setting. These strong upper crustal signatures within rocks that are otherwise rather primitive have generally been ascribed to two modes of formation: (1) significant contamination of ascending mafic magmas – either through crustal assimilation or magma mixing, and (2) partial melting of an ultramafic mantle source region that has been metasomatically modified by fluids derived from subducted materials. Each of these possibilities will be discussed below.

Contamination of mafic magma.—The Lincoln syenites show relatively high abundances of many trace elements (for example, Sr, Rb, Ce) relative to average continental crust (Taylor and McLennan, 1985), thus making significant amounts of crustal assimilation unlikely. Likewise, significant continental crustal contributions would significantly raise the SiO_2 content and dilute MgO, Ni, and Cr concentrations which

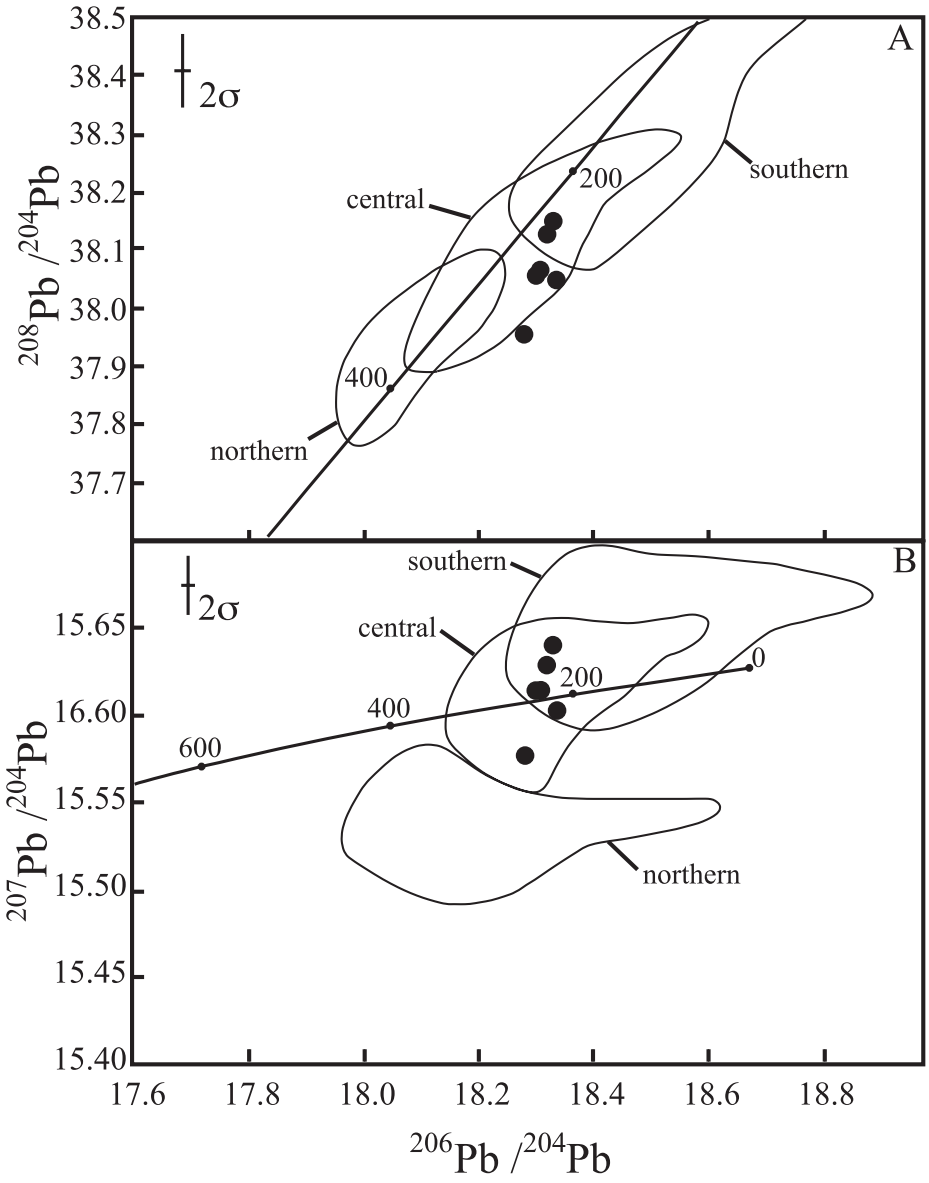

Fig. 12. Plots of Pb isotopic compositions of Lincoln syenite alkali feldspar samples: (A) $^{208}Pb/^{204}Pb$ versus $^{206}Pb/^{204}Pb$; (B) $^{207}Pb/^{204}Pb$ versus $^{206}Pb/^{204}Pb$. Plots include fields taken from Ayuso and Bevier (1991) and the model two-stage growth curve of Stacey and Kramers (1975), with tic marks in Ma. The feldspar samples show a general enrichment in $^{207}Pb/^{204}Pb$ relative to $^{206}Pb/^{204}Pb$, not typical of materials with Laurentian sources.

remain relatively primitive in these rocks (fig. 13). Additionally, the lack of a significant Eu anomaly (fig. 10) suggests that plagioclase feldspar, abundant in crustal rocks, did not participate significantly in the melting or crystallization process. Finally, macroscopic xenoliths and microscopic xenocrysts that might represent incompletely di-

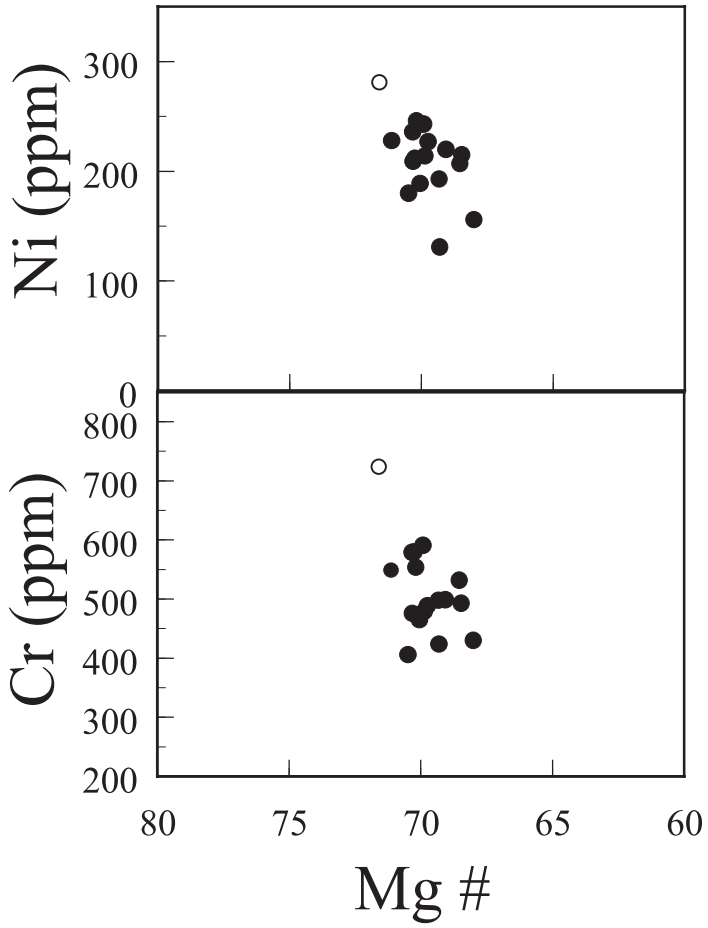

Fig. 13. Mg# vs Cr and Ni illustrating the primitive character of the Lincoln syenite

gested country rock are not abundant in the Lincoln syenite (with the exception of the immediate contact zones) and again suggest the assimilation of country rock did not play a significant role in the evolution of this magma.

While relatively fine-grained mafic enclaves are more abundant than xenoliths in the Lincoln syenite, large-scale magma mixing is not considered to have played a significant role in the geochemical evolution of these rocks. Most importantly, the fine-grained mafic enclave that could be taken to represent one of the end-member magma types, is geochemically very similar to the porphyritic syenites (ultrapotassic and indistinguishable in REE and extended element diagrams, figs. 10 and 11). Additionally, textures suggestive of magma mixing (for example, ovoid textures, rapakivi mantling, *et cetera*: see Hibbard, 1991 for a summary) have not been observed. While mixed magma systems of Late Silurian age are common in the nearby coastal Maine magmatic province (Stewart and others, 1988; Hogan and Sinha, 1989; Wiebe, 1993, 1994; Seaman and others, 1995; Ayuso and Arth, 1997; Wiebe and others, 2004), none of these rocks share mineralogical, textural or geochemical similarities with rocks of the Lincoln syenite.

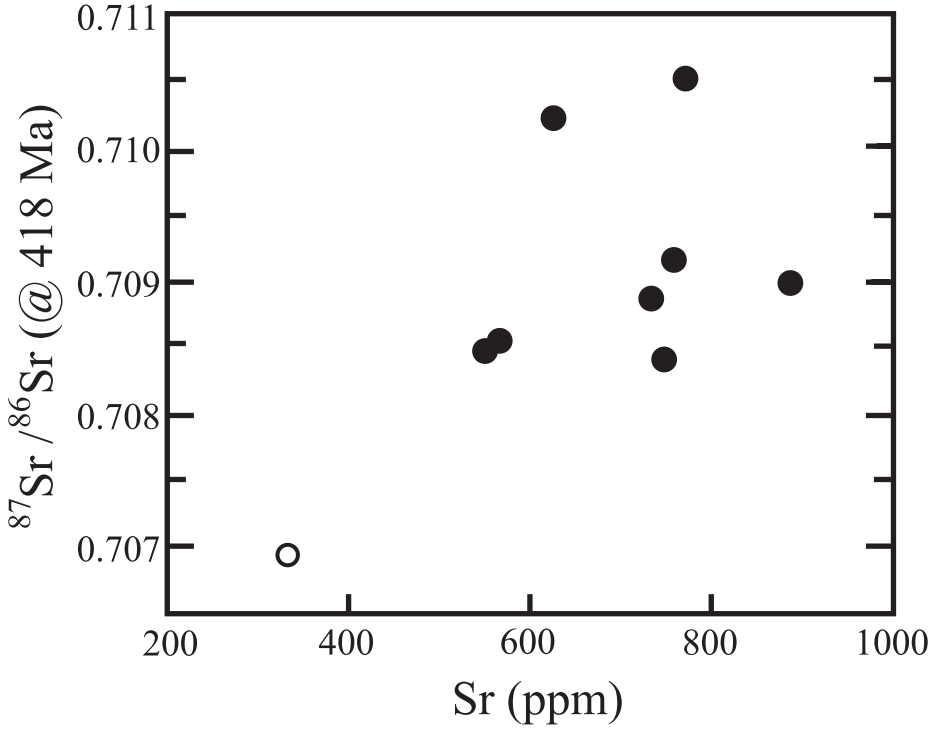

Fig. 14. Plot of initial Sr isotopic composition versus Sr concentration. The absence of correlation places strong limits on crustal assimilation as an important petrogenetic process with these rocks.

The absence of correlation between calculated initial $^{87}Sr/^{86}Sr$ and Sr content (fig. 14) indicates that the Rb/Sr isotopes are not likely to be controlled by mixing. Mixing between an enclave-like end member and something with higher $^{87}Sr/^{86}Sr$ (presumably continental crust) would require both an extremely heterogeneous crustal contaminant and a fortuitous extent of mixing, in order to derive such a cluster in Sr concentration and isotopic composition.

Similar-age gabbroic intrusions in Maine, New Brunswick and Newfoundland all record initial Nd isotopic compositions that are higher than the highest values measured here (-1.0 to +4.8; Kerr and others, 1995; Whalen and others, 1996a; Ayuso and Arth, 1997). Although Pb concentrations were determined for the Lincoln syenite samples, their mineralogy and other elemental enrichments suggest Pb would be enriched by at least tenfold over the lower crustal average of c. 4 ppm (Taylor and McLennan, 1985). Given this inference and the very high measured concentrations of Nd and Sr in the Lincoln syenite samples, limits can be placed on the extent of lower crust contamination needed to produce the measured Pb, Nd and Sr isotope signatures using mixing calculations (Langmuir and others, 1978). These calculations indicate that the proportion of lower crust needed to replicate the measured isotopic signatures would so reduce the concentrations of elements like K and Ba as to preclude this as a geologically viable mechanism.

In summary, it is highly unlikely that crustal assimilation or magma mixing played a significant role in the geochemical evolution of the Lincoln syenite. Therefore, the

unique geochemical characteristics of these rocks most likely reflect the characteristics of the source region rather than post-melting processes.

Source region subduction-related metasomatism.—A primary origin for the large ion lithophile element (LILE) abundances in the Lincoln syenite requires either unrealistically small amounts of partial melting (<< 1%) in what might be considered to be typical mantle source rocks, or more realistic amounts of partial melting in an ultramafic source region rich in LILE-bearing mineral phases. High pressure experimental studies of potassic melts that most closely resemble those of the Lincoln syenite are consistent with derivation from an ultramafic source region rich in phlogopite (Foley, 1992a). In other words, the mantle source region for the potassium-rich mafic melt acquires its enriched mantle signature prior to partial melting. The commonly accepted mechanism for this mantle enrichment is through the introduction of fluids derived from an underlying subducting slab. The upward migration of dehydration fluids results in the deposition of hydrous vein networks (rich in phlogopite) in the mantle wedge above the subducting slab (Wyllie and Sekine, 1982). Melting is postulated to begin in the veins due to the concentration of hydrous phases and incompatible elements, but quickly spreads to include the surrounding ultramafic wall rocks (Foley, 1992b). Thus, resulting partial melts will be imprinted with characteristics of both the metasomatic veins (LILE and LREE enrichment) and the surrounding ultramafic wall rocks (high MgO, Ni, Cr). The partial melting of a mantle source region unaffected by metasomatic processes can effectively be ruled out though comparisons of the Lincoln syenite trace element chemistry with that of a wide variety of OIB and MORB magmas. For example, Th is highly enriched in the Lincoln syenite relative to a mantle array defined by OIB and MORB (fig. 15A).

A number of characteristics of the Lincoln syenites are consistent with the partial melting of a metasomatized mantle source region. In particular, the abundance of LILEs in rocks otherwise primitive in composition (for example, high Mg#, Cr and Ni) requires mixed sources. Additionally, the Lincoln syenites show a striking depletion of the high field strength elements Nb and Ta: (figs. 11 and 15B) that are characteristic of arc-derived magmas (Gill, 1981; Wilson, 1989). Indeed, trace element compositions of the Lincoln syenites typically plot in "subduction fields" on commonly used tectonomagmatic discrimination diagrams (for example, fig. 15B and Rb-Th-Hf, not shown).

Finally, the majority of the Lincoln syenite samples record depleted mantle model ages (fig. 16) that are older than the generally accepted estimate of crustal extraction for Laurentian crust (McLelland and others, 1993). One possibility is that this age reflects incorporation of elements added to the lithosphere during Proterozoic subduction. The Nd isotopic data could also be satisfied by incorporation of a c. 1 Ga crustal component into the mantle any time between then and the crystallization of the syenite.

In summary, the unique geochemical characteristics of the Lincoln syenite are most consistent with the partial melting of a mantle wedge previously metasomatized by subduction derived fluids. An important point to make is that the source region heterogeneities described above can persist long after subduction driven hydration has ceased (for example, Thompson and others, 1989; O'Brien and others, 1995; Feldstein and Lange, 1999). Thus, an important petrotectonic question, to be addressed below, is whether this partial melting event was synchronous with subduction, or whether some post-subduction tectonic event triggered the melting of a previously metasomatized source region.

Magma Crystallization

Primary igneous rocks (that is those not affected by post-magmatic recrystallization) of the Lincoln syenite are mineralogically relatively simple (alkali feldspar

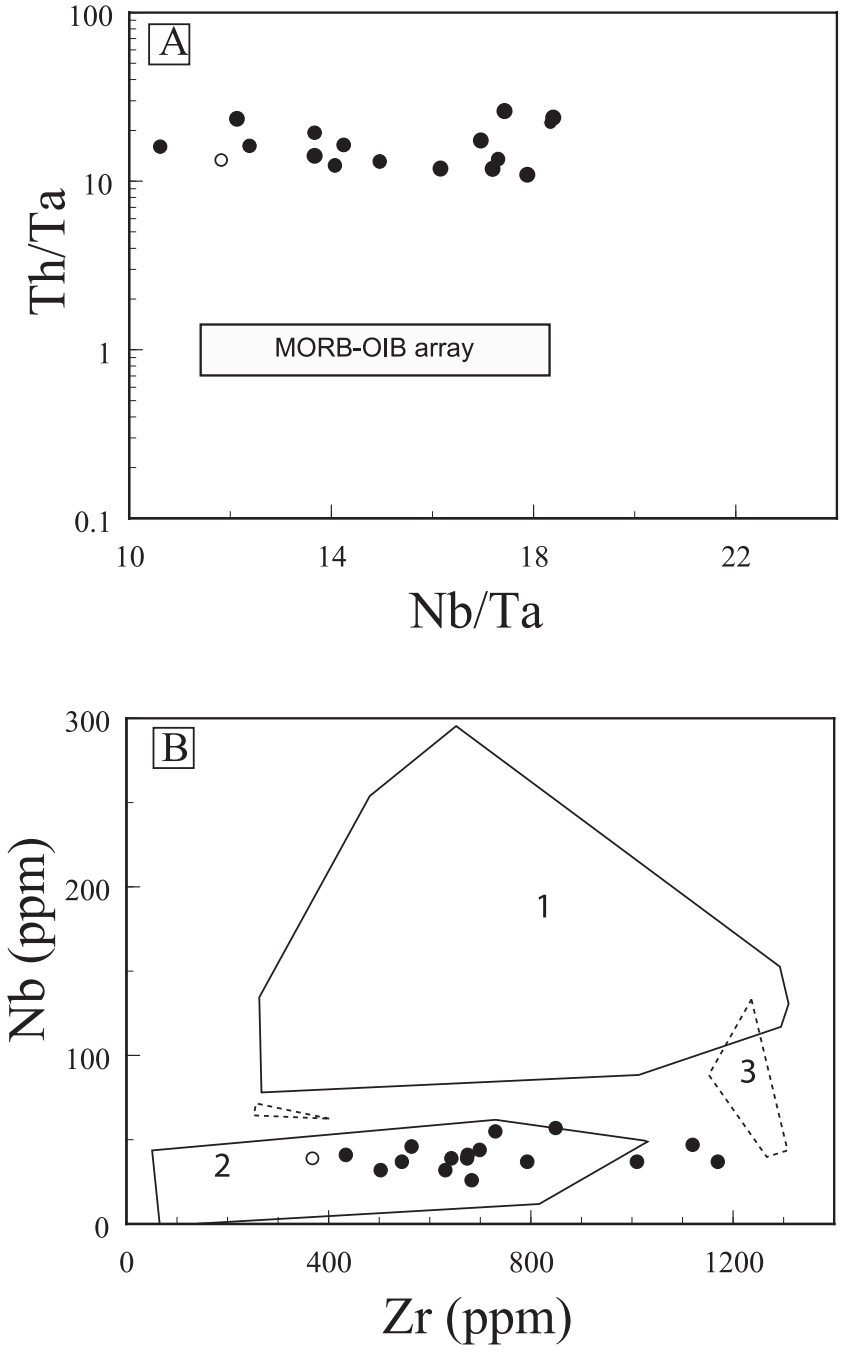

Fig. 15. (A) Nb/Ta versus Th/Ta for Lincoln Syenite samples compared to the MORB-OIB or mantle array of Pearce and others (2005). Lincoln Syenite samples are similar in their range of Nb/Ta ratios to MORB-OIB but have higher Th/Ta indicating that Th has been added to the mantle source, perhaps from a subducting slab. (B) Nd versus Zr for rocks of the Lincoln syenite. The outlined fields are for ultrapotassic igneous rocks with less than 60% SiO_2 and are adapted from Leat and others (1986) and Thompson and Fowler (1986). (1) locations remote from subduction in time and space, (2) locations closely related to subduction in space and/or time, including the first few million years following continental collisions, and (3) locations which have a remote spatial association with subduction.

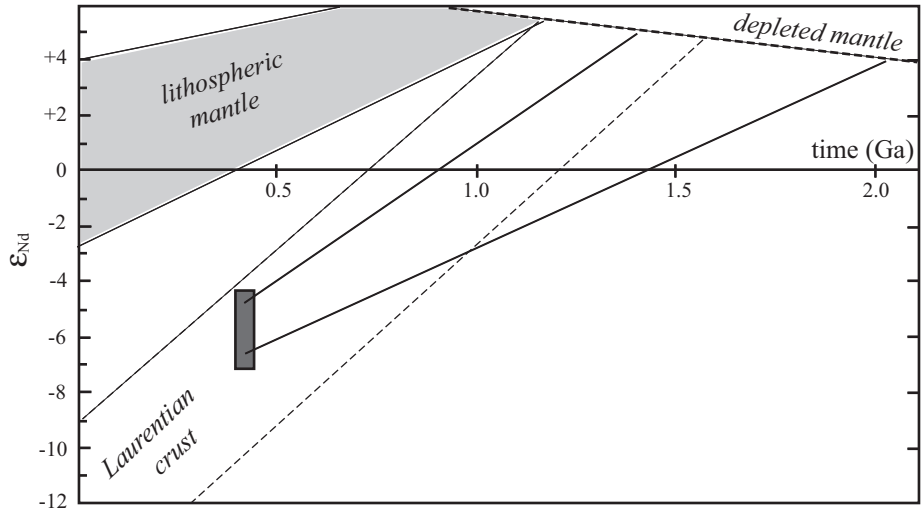

Fig. 16. Plot of Nd isotopic composition versus time. The Lincoln syenite samples are represented at their crystallization age by the box, and their present-day Sm/Nd are used to calculate model ages of extraction from the depleted mantle. Also included are data for possible subcontinental lithosphere (Foland and others, 1988; Pegram, 1990) and for Laurentian crust (McLelland and others, 1993).

megacrysts set in a groundmass dominated by alkali feldspar + clinopyroxene + orthopyroxene + biotite + oxides) and show little variability. Similarly, these rocks show surprisingly little major and trace element variability (figs. 8-11) despite attempts to sample the widest variety of rock types available. While individual minerals within the syenite are zoned, complexly in the case of the alkali feldspar megacrysts, it is believed that the fractionation of major phases played a limited role in the rocks currently exposed at the surface.

Textural evidence in combination with mineral chemistry suggests that all the phases present in the Lincoln syenite are co-genetic (that is, not xenocrysts). Normal chemical zoning patterns and rim compositions of adjacent ortho- and clinopyroxene are indicative of equilibrium conditions during crystallization (fig. 6). Alkali feldspar megacrysts show zonally arranged patterns of groundmass inclusions (fig. 4D) and coupled with barium rich cores suggest an early period of alkali feldspar nucleation and growth in the potassium-rich mafic magma. It is suggested that these megacrysts continued to grow, albeit in a changing chemical environment, throughout the crystallization of the syenite. This is supported by the chemical similarity of alkali feldspar megacryst outer margins with matrix alkali feldspar compositions (fig. 5). Alkali feldspar crystallization in mafic ultrapotassic magmas is not uncommon (for example, Perini and others, 2003).

One of the more intriguing aspects of the Lincoln syenite is the paucity of plagioclase feldspar in an igneous rock of intermediate composition. Several experimental studies on a variety of melt compositions (Eggler, 1972; Sisson and Grove, 1993; Moore and Charmichael, 1998) have shown that water is an effective agent for the suppression of plagioclase feldspar crystallization. Indeed, the presence of significant amounts of water (> 3 wt. %) in the magma may provide an explanation for other characteristics of the Lincoln syenite. The nucleation of alkali feldspar is also inhibited by high water contents (Fenn, 1977) and thus a relatively small number of nucleation sites coupled with rapid alkali migration in the melt provides a mechanism for the

TABLE 4

Comparison of Lincoln syenite and Parks Pond geochemistry

Wt. %	Lincoln Syenite* (average of 16 samples)	Parks Pond Pluton** (average of 8 samples)
SiO_2	56.9	57.6
TiO_2	1.4	1.2
Al_2O_3	11.3	11.9
Fe_2O_3(t)	7.0	6.8
MnO	0.1	0.1
MgO	8.2	8.6
CaO	4.6	5.0
Na_2O	2.0	1.5
K_2O	6.6	5.6
P_2O_5	0.8	0.7
Ba (ppm)	1759	1448
Cr (ppm)	503	425
Ni (ppm)	207	174

*Lincoln syenite average does not include data from the mafic enclave.

**Parks Pond data provided by John Hogan (written communication, 2005), but the data is summarized in Hogan and Sinha (1989) and briefly discussed in Eriksson and Wones (1983).

growth of large alkali feldspar megacrysts (Swanson, 1977). Additionally, relatively high water contents (3 to 5 wt. %) aid in the crystallization of Mg-rich biotite (found in the Lincoln syenite) in potassic melts (Esperanca and Holdoway, 1987; Righter and Carmichael, 1996). The inferred importance of water in the crystallization of the Lincoln syenite is also consistent with derivation from a source region rich in slab-derived metasomatic veins.

In summary, textural, mineralogical and geochemical evidence suggests all the phases present in the Lincoln syenite are co-genetic. The presence of significant amounts of water in the magma likely suppressed plagioclase feldspar crystallization, facilitated the crystallization of Mg-rich biotite, and ultimately resulted in the nucleation and growth of large alkali feldspar megacrysts.

REGIONAL TECTONIC IMPLICATIONS

Any petrotectonic model for the origin of the Lincoln syenite should account for the relatively restricted nature, both in time and in space, of mafic ultrapotassic magmatism in the region. Rocks of the Lincoln syenite are distributed in roughly an orogen-parallel orientation for a distance of nearly 75 km in Maine. A geochemically similar rock body, the Parks Pond pluton (Eriksson and Wones, 1983; Hogan and Sinha, 1989), is located in a similar structural position (along the northwestern margin of the Fredericton belt) approximately 80 km northeast of the northern most extent of the Lincoln syenite (see the inset map in fig. 1). Although significantly smaller (< 10 km^2), the Parks Pond pluton appears to be similar in age to the Lincoln syenite (410 ± 4 Ma: unpublished U-Pb zircon age quoted in Hogan and Sinha, 1989). More importantly, the geochemical characteristics of the Parks Pond pluton are strikingly similar to that of the Lincoln Syenite (Hogan and Sinha, 1989; summarized in table 4). Taken collectively, these observations argue for a similar petrogenesis. The correlation of these two ultrapotassic intrusions extends the distribution of this style of Late Silurian-Early Devonian magmatism to an orogen parallel distance of over 150 km.

As discussed above, the geochemical characteristics of the Lincoln syenite (and by association the Parks Pond pluton) are most likely due to the partial melting of a metasomatized lithospheric mantle source region. It is generally accepted that this metasomatism was driven by the introduction of hydrous vein material derived from rising fluids above a subducting lower plate. Rocks from known tectonic settings that display similar geochemical characteristics (ultrapotassic, LILE enriched, mafic, arc trace element signatures, *et cetera*) show a strong connection with subduction-related processes (Peccerillo, 1985; Edwards and others, 1991; Conticelli and Peccerillo, 1992; O'Brien and others, 1995; Carmichael and others, 1996; Feldstein and Lange, 1999; Farmer and others, 2002; Gertisser and Keller, 2003; Williams and others, 2004; Zang and others, 2005). Thus, knowledge of the unique tectonic setting required for the generation of the ultrapotassic magmas in Maine provides an important independent constraint on Silurian-Devonian (Acadian) tectonic models of the region.

Although direct evidence of Late Silurian-Early Devonian subduction processes in New England is generally lacking (for example, no ophiolite belt, zone of high-pressure metamorphism, or belt of unequivocal igneous arc rocks), all modern tectonic models of Acadian orogenesis involve some component of oceanic subduction (for example, Osberg, 1978; Bradley, 1983; Osberg and others, 1989; Ludman and others, 1993; van Staal and de Roo, 1995; Eusden and others, 1996; Tucker and others, 2001; Moench and Aleinikoff, 2003). Indeed, paleogeographic considerations alone (Neuman and others, 1989; Berry and Osberg, 1989; Nowlan and Neuman, 1995) require the existence of a wide marine basin separating the Laurentian margin and peri-Gondwanan terranes (for example, Avalon) through Early Silurian time. The geochemical characteristics of the Lincoln syenite (and by association the Parks Pond pluton) require a significant period of subduction driven metasomatism prior to partial melting in Late Silurian-Early Devonian time. In detail, two key questions remain: (1) what was the polarity of this subduction – to the northwest (present day coordinates) beneath the Laurentian continental margin, or to the southeast beneath converging peri-Gondwanan terranes? (2) When was this subduction active relative to the Late Silurian-Early Devonian partial melting event that produced the ultrapotassic magmas? As noted earlier, the source region heterogeneities (metasomatic veins in mantle peridioties) required for the generation of ultrapotassic mafic magmas can persist long after subduction driven hydration has ceased (for example, Thompson and others, 1989; O'Brien and others, 1995; Feldstein and Lange, 1999). In other words, the "subduction fingerprint" of the ultrapotassic intrusions in Maine could have been inherited from subduction events millions of years prior to the generation of the magma.

Some comment on the general tectonic settings of geochemically similar igneous rocks globally is warranted. With the notable exceptions of Indonesia (Edwards and others, 1991; Gertisser and Keller, 2003) and western Mexico (Carmichael and others, 1996) where subduction and calc-alkaline magmatism are synchronous with ultrapotassic magmatism, nearly all occurrences of this style of igneous activity are associated with extensional processes superimposed on rocks earlier affected by subduction-driven metasomatism. These settings include the Plio-Pleistocene ultrapotassic igneous province of Italy (Conticelli and Peccerillo, 1992; Conticelli and others, 2002), Pliocene ultrapotassic magmatism in the Sierra Nevada of California (Feldstein and Lange, 1999; Farmer and others, 2002), Eocene ultrapotassic magmatism in Montana (O'Brien and others, 1991, 1995), Cenozoic ultrapotassic lavas in Tibet (Turner and others, 1996; Williams and others, 2004; Guo and others, 2006), and Mesozoic ultrapotassic intrusions in eastern China (Yang and others, 2005; Zhang and others, 2005). In all of these examples, tectonic models call for a period of continental margin subduction

followed by extension, frequently triggered by lithospheric delamination or slab break off.

The Lincoln syenite intrudes both Middle to Late Ordovician rocks of the Liberty-Orrington belt and Silurian rocks of the Fredericton belt suggesting these two lithotectonic terranes were proximal to one another in Late Silurian-Early Devonian time. While the Fredericton belt is composed primarily of metamorphosed turbidites, the Liberty-Orrington belt (and correlative rocks to the southwest and northeast) is composed of a variety of metamorphosed volcanic and volcanogenic sedimentary rocks (Hussey and Berry, 2002; West and others, 2003) interpreted to represent a Middle to Late Ordovician arc to back arc sequence (van Staal and others, 2003; West and others, 2004). Additionally, studies of faunal provinciality (Neuman and others, 1989; Nowlan and Neuman, 1995) require an oceanic barrier existed through Early Silurian time between rocks now juxtaposed along the eastern margin of the northern Appalachians. Therefore, despite the lack of direct evidence for subduction (for example, ophiolite and/or high-pressure metamorphic belt) there are several independent lines of evidence that argue for earlier episodes of Paleozoic subduction in the region.

Mataragio and Hogan (2004) in a recent survey of geochemical and isotopic data from Silurian-Devonian plutonic rocks in eastern Maine indicate that Silurian plutonic rocks record both subduction and extensional tectonic settings, while Devonian plutonic rocks indicate a tectonic setting other than subduction and likely formed as a result of crustal thickening. Indeed while recent tectonic models for the region based on stratigraphic, structural, and petrologic constraints involve Late Ordovician-Silurian subduction (for example, Ludman and others, 1993; van Staal and der Roo, 1995; Eusden and others, 1996; Tucker and others, 2001; Moench and Aleinikoff, 2003), most models have subduction ending by the end of the Silurian period (although convergence continued). This information, combined with the fact that ultrapotassic magmatism in Maine is not temporally or spatially associated with abundant calc-alkaline magmatic rocks, strongly suggests that the subduction-driven metasomatism preceded generation of the mafic ultrapotassic magmas in this region. We therefore adopt a tectonic model similar to that proposed for other regions where these types of rocks are found (see references above). Specifically, earlier subduction events resulted in metasomatism of an overlying mantle wedge and this was followed by a period of extension. Extensional processes would not only result in the upwelling of hot asthenospheric material facilitating melting of vein assemblages within the mantle wedge, but it would also provide pathways to the middle and upper crust.

Whereas subduction has been an integral part of Acadian tectonic models, much controversy has centered on the polarity of the subduction and in particular whether there existed more than one subduction zone (see Robinson and others, 1998 for a review). Many Acadian tectonic models call upon dual-vergent subduction in the Silurian: one slab dips northwest beneath North America and the other dips southeast beneath converging peri-Gondwanan terranes (for example, Bradley, 1983; Ludman and others, 1993; Eusden and others, 2000; Moench and Aleinikoff, 2003).

Isotopic data from the Lincoln syenite are most consistent with derivation from basement rocks that underlie central Maine (that is Gander, Bronson Hill or simply central Maine basement) rather than more easterly terranes (that is Avalon). Specifically, Pb isotopic signatures are similar to igneous rocks in central Maine (fig. 12 and Tomascak and others, 2005), and relatively low $\varepsilon_{Nd}(T)$ values are consistent with interactions with Gander crust rather than Avalonian (Whalen and others, 1996b; Samson and others, 2000; West and others, 2004). Nearly all Acadian tectonic models involve the closure of an ocean basin that existed between Laurentia plus previously accreted Ordovician arc terranes (for example, Bronson Hill, Gander, *et cetera*) and

more easterly Gondwanan terranes (that is Avalon). Since the isotopic characteristics of the Lincoln syenite are most consistent with basement rocks on the western side (present day coordinates) of this ocean basin, it seems most likely that the subduction required for metasomatism of the mantle source region must have been directed beneath these rocks. However, it is important to reiterate that the isotopic data from the Lincoln syenite do not allow us to discern whether this subduction driven metasomatism was operative during the Silurian or some earlier time in the Paleozoic (for example, during the creation of the Ordovician arc terranes).

Preferred Tectonic Model

We have reviewed previously proposed models of Acadian orogenesis and compared them with the rather restricted tectonic settings associated with rocks that are geochemically and isotopically similar to rocks of the Lincoln syenite. The rather restricted nature of ultrapotassic mafic magmatism in Maine must also be considered. Specifically evidence for this type of magmatism is limited to a brief time interval (latest Silurian to earliest Devonian time), yet is distributed in a relatively long (~ 150 km), linear orogen-parallel belt.

The following tectonic settings for the ultrapotassic magmatism in Maine are not considered viable: (1) ultrapotassic magmatism contemporaneous with subduction, as is the case in Indonesia (Edwards and others, 1991; Gertisser and Keller, 2003) and western Mexico (Carmichael and others, 1996). Both of these areas are characterized by voluminous contemporaneous calc-alkaline magmatism that is not found in association with the ultrapotassic rocks in Maine. (2) Ultrapotassic magmatism associated with the early stages of transcurrent fault development (for example, Sloman, 1989; Vaughan and Scarrow, 2003). The parallelism of the ultrapotassic magmatism in Maine with the regionally extensive Norumbega fault system (fig. 1) makes this association superficially attractive. However, the timing of early dextral strike-slip activity associated with the Norumbega fault system (West and Hubbard, 1997; West, 1999; Ludman and others, 1999) is significantly younger (20 to 30 Ma) than the ultrapotassic magmatism and thus a connection is considered unlikely. (3) Melting associated with a mantle plume, as has been proposed for Cretaceous mafic potassic magmatism in southeastern Brazil (Gibson and others, 1999). Potassic magmatism in these settings tends to be more voluminous and more mafic (kimberlites, lamproites) than what is found in Maine.

Remaining tectonic settings proposed for the style of ultrapotassic magmatism most similar to that in Maine center on brief periods of intense lithospheric extension triggered by slab-break off or lithospheric delamination following collision. One example is post-collisional potassic magmatism in Tibet (Turner and others, 1996; Williams and others, 2004), where both convective removal of the subcontinental lithospheric mantle and slab break-off have been proposed to explain ultrapotassic magmatism. Similarly, lithospheric delamination has been proposed to have triggered late Cenozoic ultrapotassic magmatism in the Sierra Nevada, California (Farmer and others, 2002) and Mesozoic ultrapotassic magmatism in eastern China (Yang and others, 2005). Common to each of these tectonic settings is a relatively brief period of lithospheric heating that triggered partial melting of a previously subduction-modified lithospheric mantle. Both slab detachment and lithospheric delamination would result in the rapid upwelling of hot asthenospheric material and partial melting of the overlying lithosphere.

Previously proposed models of Acadian orogenesis that involve some component of west dipping subduction seem most compatible with the slab detachment/lithospheric delamination settings discussed above. Figure 17 represents schematic Acadian plate tectonic models consistent with the observations. Model A, modified

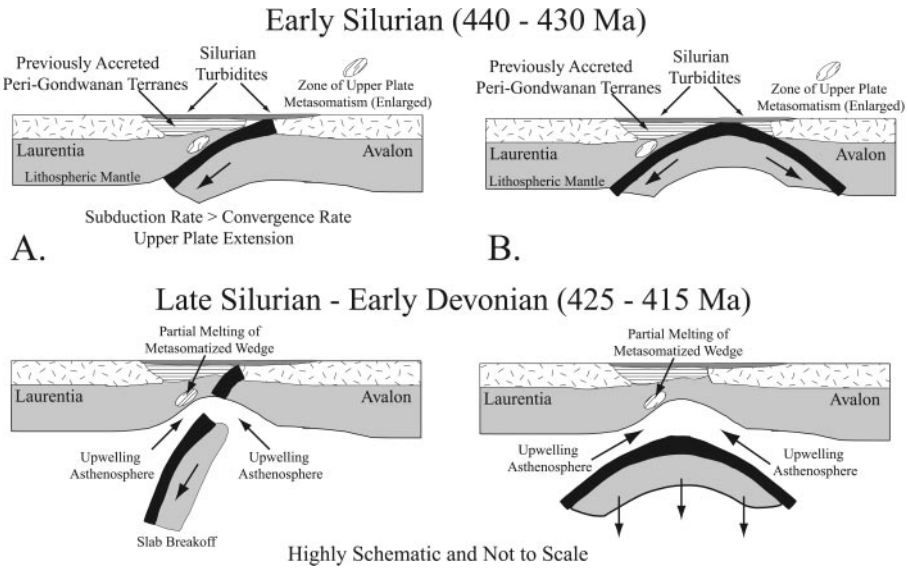

Fig. 17. Highly schematic models of Silurian to Early Devonian orogenesis oriented perpendicular to strike across south-central Maine. (A) A single, west directed subduction model modified from van Staal and de Roo (1995). In this model, slab break-off following collision triggers extension and partial melting of a previously metasomatized mantle wedge. (B) A two-subduction model modified from Bradley, (1983), Ludman and others (1993), Eusden and others (1996), and Moench and Aleinikoff (2003). As discussed by Moench and Aleinikoff (2003) occlusion of the opposed subduction zones would lead to sinking of the previously subducted oceanic lithosphere and asthenospheric replacement. This would also result in partial melting of a previously metasomatized mantle wedge. Note, "previously accreted peri-Gondwanan terranes" labeled in both models includes Gander along with other peri-Gondwanan terranes that were accreted to Laurentia in the Early Silurian (van Staal and others, 1998).

from van Staal and de Roo (1995), involves only westerly directed subduction during the Early Silurian. Any model involving westward subduction beneath Laurentia during the Early Silurian must provide an explanation for the lack of arc volcanic rocks of this age in central New England. Eusden and others (2000) have suggested that the angle of subduction was too shallow to initiate partial melting and arc volcanism. An alternate explanation, one that is consistent with other geological characteristics of the region, is that westward subduction was retreating rather than advancing (van Staal and de Roo, 1995). This type of subduction boundary, discussed by Royden (1993), forms where the overall rate of plate convergence is less than the rate of subduction. This scenario results in regional extension in the overriding plate and a protracted period of pre- to syn-collisional flysch deposition in the adjacent foredeep. This provides an explanation for the thick accumulation of Silurian turbidites in the central Maine sequence, some of which are chaotically deformed and have been interpreted as subduction mélange associated with a west dipping subduction zone (Eusden and others, 1996). The net effect is that all this extension and turbidite deposition may have flooded and buried any Silurian arc rocks that were present in an overriding Laurentian plate.

This westward subduction of oceanic lithosphere, whether retreating or not, would have resulted in hydration-driven metasomatism in the overriding lithospheric mantle wedge – an essential precursor to the Late Silurian-Early Devonian ultrapotassic magmatism in Maine. Following the model of van Staal and de Roo (1995), it is suggested that, during the early stages of collision, plate rupture or slab break off

occurred due to increased density of the descending slab from the conversion to eclogite. The detachment of this oceanic lithosphere would have resulted in increased amounts of extension and replacement by hot asthenospheric material. Both of these processes would have served to drive a linear zone of partial melting in the overlying metasomatically altered lithospheric mantle wedge. The earliest stages of this partial melting would be concentrated in the hydrous LILE enriched veins and result in the generation of hydrous ultrapotassic magmas. This rise of hot asthenospheric material to relatively high structural levels would have also been a driving agent for the extensive regions of low-pressure metamorphism so characteristic of central and southern Maine (see Guidotti, 1989 for a summary). Continued convergence, and the migrating Acadian deformational front demonstrated by Bradley and others (2000) following slab break off would likely have been driven by more outboard collisions (for example, Meguma). A similar model involving slab breakoff has been proposed to explain the distribution of Silurian-Devonian high-potassium calc-alkaline magmas in the Caledonian orogenic belt of Ireland and Scotland (Atherton and Ghani, 2002).

Model B involves two-sided subduction (Bradley, 1983; Ludman and others, 1993; Eusden and others, 2000; Moench and Aleinikoff, 2003). Processes similar to those described above (for example, retreating subduction, mantle wedge metasomatism) would have been operative on the western side of this two-sided model. As discussed by Moench and Aleinikoff (2003), continued convergence driven by two-sided subduction eventually results in an "occlusion" of the opposed subduction zones. The net result of this occlusion would be the juxtapositioning of two metasomatically altered mantle wedges above a sinking slab of oceanic lithosphere. This sinking oceanic lithosphere, beneath the Fredericton belt in the model of Moench and Aleinikoff (2003), would again be replaced by hot asthenospheric mantle which would drive partial melting in the overlying metasomatically altered lithospheric mantle wedges.

It should be noted that the single east-dipping subduction model favored by Tucker and others (2001) also incorporates a component of lithospheric delamination that would introduce anomalously hot asthenospheric material to high structural levels. However, it is difficult to reconcile the isotopic signature of the Lincoln syenite (a central Maine or Gander isotopic signature) with partial melting of a mantle wedge formed above an east dipping subduction zone (which would likely result in Avalonian isotopic signatures).

Regardless of the tectonic model, the geochemical and isotopic characteristics of the Lincoln syenite (and by association the Parks Pond pluton) are best explained by partial melting of a subduction-driven metasomatically altered mantle wedge. In addition, studies of similar rocks from known tectonic settings call on a period of lithospheric extension superimposed on this mantle wedge in order to facilitate partial melting and eventual ultrapotassic magma ascent.

CONCLUSIONS

Several important conclusions can be drawn from our detailed petrologic and geochemical study of the Lincoln syenite in Maine:

(1) The rocks are geochemically distinct, characterized by being intermediate in SiO_2 content, ultrapotassic (6–7 wt % K_2O), and yet quite primitive in terms of Mg#, and Ni and Cr contents. Additionally, the rocks are enriched in large ion lithophile elements relative to high field strength elements, have elevated abundances of light rare earth elements, and have high initial $^{87}Sr/^{86}Sr$ ratios.

(2) The unusual geochemical and isotopic characteristics of these rocks can be attributed to the partial melting of a mantle wedge previously metasomatized by subduction derived fluids.

(3) Magma crystallization was greatly influenced by significant amounts of water that suppressed plagioclase feldspar crystallization and facilitated the growth of large alkali feldspar megacrysts.
(4) Correlation with the geochemically similar Parks Pond pluton extends the distribution of Late Silurian-Early Devonian ultrapotassic magmatism in Maine to an orogen-parallel distance of over 150 km.
(5) Any geodynamic model of Acadian orogenesis in this region must accommodate the unique petrotectonic setting required for the genesis of these ultrapotassic magmas. We favor a tectonic model involving some component of westward directed subduction followed by Late Silurian-Early Devonian slab breakoff or delamination. Both models provide a mechanism for the decompression melting of previously metasomatized mantle wedge rocks.

ACKNOWLEDGMENTS

Funding for this work was provided by the National Science Foundation (EAR-027263) and the Maine Geological Survey through the STATEMAP program. Discussions with Henry Berry, John Hogan, and Arthur Hussey have been most helpful. John Hogan is additionally thanked for providing geochemical data from the Parks Pond pluton collected by S. C. Eriksson while at Virginia Tech. Dan Barker (University of Texas) is also thanked for his preliminary work on mineral chemistry. PBT thanks the Dean of Arts and Sciences at SUNY-Oswego for support of student research, Laura Bianchi and Kimberly Finnigan for assistance in the laboratory, and S. D. Samson for his hospitality and assistance at Syracuse University. The authors thank Mike Dorais, David Stewart, and Robert Wintsch for constructive reviews of the manuscript.

References

Atherton, M. P., and Ghani, A. A., 2002, Slab breakoff: a model for Caledonian, Late Granite syn-collisional magmatism in the orthotectonic (metamorphic) zone of Scotland and Donegal, Ireland: Lithos, v. 62, p. 65–85.

Ayuso, R. A., and Arth, J. G., 1997, The Spruce Head composite pluton: an example of mafic to silicic Salinian magmatism in coastal Maine, northern Appalachians, *in* Sinha, A. K., Whalen, J. B., and Hogan, J. P., editors, The nature of magmatism in the Appalachian orogen: Geological Society of America Special Memoir 191, p. 19–43.

Ayuso, R. A., and Bevier, M. L., 1991, Regional differences in Pb isotopic compositions of feldspars in plutonic rocks of the northern Appalachian mountains, U.S.A. and Canada: a geochemical method of terrane correlation: Tectonics, v. 10, p. 191–212.

Barton, M., and Sidle, W. C., 1994, Petrological and geochemical evidence for granitoid formation: the Waldoboro pluton complex, Maine: Journal of Petrology, v. 35, p. 1241–1274.

Bastin, E. S., 1906, Some unusual rocks from Maine: Journal of Geology, v. 14, p. 173–180.

Berry, H. N., IV, and Osberg, P. H., 1989, A stratigraphic synthesis of eastern Maine and western New Brunswick, *in* Studies in Maine Geology. v. 2, Tucker, R. D., and Marvinney, R. G., editors: Augusta, Maine, Maine Geological Survey, p. 1–29.

Bradley, D. C., 1983, The tectonics of the Acadian orogeny in New England and adjacent Canada: Journal of Geology, v. 91, p. 381–400.

Bradley, D. C., Tucker, R. D., Lux, D. R., Harris, A. G., and McGregor, D. C., 2000, Migration of the Acadian Orogen and foreland basin across the Northern Appalachians: United States Geological Survey Professional Paper 1624, 79 p.

Carmichael, I. S. E., Lange, R. A., and Luhr, J. F., 1996, Quaternary minettes and associated volcanic rocks of Mascota, western Mexico: a consequence of plate extension above a subduction modified mantle wedge: Contributions to Mineralogy and Petrology, v. 124, p. 302–333.

Coish, R. A., and Sinton, C. W., 1992, Geochemistry of mafic dikes in the Adirondack mountains: implications for the constitution of Late Proterozoic mantle: Contributions to Mineralogy and Petrology, v. 110, p. 500–514.

Conticelli, S., and Peccerillo, A., 1992, Petrology and geochemistry of potassic and ultrapotassic volcanism in central Italy: petrogenesis and inferences on the evolution of mantle sources: Lithos, v. 28, p. 221–240.

Conticelli, S., D'Antonio, M., Pinarelli, L., and Civetta, L., 2002, Source contamination and mantle heterogeneity in the genesis of Italian potassic and ultrapotassic volcanic rocks: Sr-Nd-Pb isotopic data from the Roman Province and southern Tuscany: Mineralogy and Petrology, v. 74, p. 189–222.

Edwards, C., Menzies, M., and Thirlwall, M., 1991, Evidence from Muriah, Indonesia for the interplay of supra-subduction zone and intraplate processes in the genesis of potassic alkaline magmas: Journal of Petrology, v. 32, p. 555–592.
Eggler, D. H., 1972, Water-saturated and undersaturated melting relations in a Paricutin andesite and an estimate of water content in natural magma: Contributions to Mineralogy and Petrology, v. 34, p. 261–271.
Elders, W. A., 1969, Zoned alkali feldspars from the Lincoln Sill syenite, Maine: Geological Society of America Abstracts with Programs, p. 271–273.
Eriksson, S. C., and Wones, D. R., 1983, The Parks Pond pluton, eastern Maine: evidence for cratonization or orogenic activity: Geological Society of America Abstracts with Programs, v. 15, p. 118.
Esperanca, S., and Holloway, J. R., 1987, On the origin of some mica-lamprophyres: experimental evidence from a mafic minette: Contributions to Mineralogy and Petrology, v. 95, p. 207–216.
Eusden, J. D., Jr., Garesche, J., Johnson, A., Maconochie, J., Peters, S., Rosbrook, J., and Widmann, B., 1996, Stratigraphy and ductile structure of the Presidential Range, New Hampshire: Tectonic implications for the Acadian orogeny: Geological Society of America Bulletin, v. 108, p. 417–436.
Eusden, J. D., Jr., Guzofski, C. A., Robinson, A. C., and Tucker, R. S., 2000, Timing of the Acadian orogeny in northern New England: Journal of Geology, v. 108, p. 219–232.
Farmer, G. L., Glazner, A. F., and Manley, C. R., 2002, Did lithospheric delamination trigger late Cenozoic potassic volcanism in the southern Sierra Nevada, California?: Geological Society of America Bulletin, v. 114, p. 754–768.
Feldstein, S. N., and Lange, R. A., 1999, Pliocene potassic magmas from the Kings River region, Sierra Nevada, California: Evidence for melting of a subduction modified mantle: Journal of Petrology, v. 40, p. 1301–1320.
Fenn, P. M., 1977, The nucleation and growth of alkali feldspars from hydrous melts: The Canadian Mineralogist, v. 15, Part 2, p. 135–161.
Foland, K. A., Raczek, I., Henderson, C. M. B., Hofmann, A. W., 1988, Petrogenesis of the magmatic complex at Mount Ascutney, Vermont, USA: Contributions to Mineralogy and Petrology, v. 98, p. 408–416.
Foley, S., 1992a, Petrological characterization of the source components of potassic magmas: geochemical and experimental constraints: Lithos, v. 28, p. 187–204.
——— 1992b, Vein-plus-wall-rock melting mechanisms in the lithosphere and the origin of potassic alkaline magmas: Lithos, v. 28, p. 435–453.
Foley, S. F., Venturelli, G., Green, D. H., and Toscani, L., 1987, The ultrapotassic rocks: Characteristics, classification, and constraints for petrogenetic models: Earth Science Reviews, v. 24, p. 81–134.
Gertisser, R., and Keller, J., 2003, Trace element and Sr, Nd, Pb and O isotope variations in medium-K and high-K volcanic rocks from Merapi volcano, central Java, Indonesia: Evidence for the involvement of subducted sediments in Sunda Arc magma genesis: Journal of Petrology, v. 44, p. 457–489.
Gibson, S. A., Thompson, R. N., Leonardos, O. H., Dickin, A. P., and Mitchell, J. G., 1999, The Late Cretaceous impact of the Trindade mantle plume: Evidence from large-volume, mafic, potassic magmatism in SE Brazil: Journal of Petrology, v. 36, p. 189–229.
Gill, J. B., 1981, Orogenic Andesites and Plate Tectonics: Berlin, New York, Springer-Verlag Publishers, 390 p.
Gou, Z., Wilson, M., Liu, J., and Mao, Q., 2006, Post-collisional, potassic and ultrapotassic magmatism of the northern Tibetan Plateau: Constraints on characteristics of the mantle source, geodynamic setting and uplift mechanisms: Journal of Petrology, v. 47, n. 6, p. 1177–1220.
Grover, T. W., 2007, Bedrock geology of the North Whitefield 7.5' quadrangle, Maine: Maine Geological Survey Map Scale = 1:24,000.
Guidotti, C. V., 1989, Metamorphism in Maine, *in* Tucker, R. D., and Marvinney, R. G., editors, Studies in Maine Geology, Volume 3, Igneous and Metamorphic Petrology: Augusta, Maine, Maine Geological Survey, p. 1–17.
Hibbard, M. J., 1991, Textural anatomy of twelve magma mixed granitoid systems, *in* Enclaves and Granite Petrology, Didier, J., and Barbarin, B., editors: Amsterdam, Elsevier Publishers, p. 431–444.
Hogan, J. P., and Sinha, A. K., 1989, Compositional variation of plutonism in the coastal Maine magmatic province: mode of origin and tectonic setting, *in* Studies in Maine Geology. v. 4. Tucker, R. D., and Marvinney, R. G., editors: Augusta, Maine, Maine Geological Survey, p. 1–33.
Hussey, A. M., II, and Berry, H. N., IV, 2002, Bedrock geology of the Bath 1:100,000 map sheet, coastal Maine: Maine Geological Survey Bulletin 42, 50 p.
Hussey, A. M., II, and Marvinney, R. G., 2002, Bedrock geology of the Bath 1:100,000 quadrangle, Maine: Maine Geological Survey, Geologic Map 02-152.
Kerr, A., Jenner, G. A., and Fryer, B. J., 1995, Sm-Nd isotope geochemistry of Precambrian to Paleozoic granitoid suites and the deep-crustal structure of the southeast margin of the Newfoundland Appalachians: Canadian Journal of Earth Sciences, v. 32, p. 224–245.
Knight, D. R., and Gaudette, H. E., 1991, Geology and petrology of the Lincoln sill and related rocks, coastal Maine, *in* Ludman, A., editor, Geology of the Coastal Lithotectonic block and neighboring terranes, eastern Maine and southern New Brunswick: Princeton, Maine, September 27–29, 1991, New England Intercollegiate Geological Conference Guidebook, 83rd Annual Meeting, p. 323–337.
Langmuir, C. H., Vocke, R. D., Hanson, G. N., and Hart, S. R., 1978, General mixing equation with applications to Iceland basalts: Earth and Planetary Science Letters, v. 37, p. 380–392.
Leat, P. T., Thompson, R. N., Morrison, M. A., Hendry, G. L., and Trayhorn, S. C., 1986, Geodynamic significance of post-Variscan intrusive and extrusive potassic magmatism in SW England: Transactions of the Royal Society of Edinburgh: Earth Sciences, v. 77, p. 349–360.

Le Bas, M. J., Le Maitre, R. W., Streckeisen, A., and Zanettin, B., 1986, A chemical classification of volcanic rocks based on the total alkali - silica (TAS) diagram: Journal of Petrology, v. 27, p. 745–750.
Le Maitre, R. W., editor, 2002, Igneous rocks: A classification and glossary of terms, Recommendations of the International Union of Geological Sciences Subcommission on the Systematics of Igneous Rocks: Cambridge, England, Cambridge University Press, 236 p.
Long, P. E., and Luth, W. C., 1986, Origin of K-feldspar megacrysts in granitic rocks: Implications of a partitioning model for barium: American Mineralogist, v. 71, p. 367–375.
Ludman, A., Hopeck, J. T., and Brock, P. C., 1993, Nature of the Acadian orogeny in eastern Maine, *in* Roy, D. C., and Skehan, J. W., editors, The Acadian Orogeny: Recent Studies in New England, Maritime Canada, and the Autochthonous Foreland: Geological Society of American Special Paper 275, p. 67–84.
Ludman, A., Lanzirotti, A., Lux, D. R., and Chunzeng, W., 1999, Constraints on the timing and displacement of multistage shearing in the Norumbega fault system, eastern Maine, *in* Ludman, A., and West, D. P., Jr., editors, Norumbega fault system of the northern Appalachians: Geological Society of America Special Paper 331, p. 179–194.
Mataragio, J. P., and Hogan, J. P., 2004, Unraveling the mid-Paleozoic magmatism in coastal Maine and its implications for crustal growth: International Basement Tectonics Conference, v. 17, p. 47–49.
McLelland, J. M., Daly, J. S., and Chiarenzelli, J., 1993, Sm-Nd and U-Pb isotopic evidence of juvenile crust in the Adirondack lowlands and implications for the evolution of the Adirondack Mts.: Journal of Geology, v. 101, p. 97–105.
Merlet, C., 1992, Quantitative electron probe microanalysis: new accurate $\phi(\rho z)$ description: Mikrochimica Acta Supplementum, v. 12, p. 107–115.
Mezger, K., Hanson, G. N., and Bohlen, S. R., 1989, High-precision U-Pb ages of metamorphic rutile: application to the cooling history of high-grade terranes: Earth and Planetary Science Letters, v. 96, p. 106–118.
Moench, R. H., and Aleinikoff, J. N., 2003, Stratigraphy, geochronology, and accretionary terrane settings of two Bronson Hill arc sequences, northern New England: Physics and Chemistry of the Earth, v. 28, p. 113–160.
Moore, G. M., and Carmichael, I. S. E., 1998, The hydrous phase equilibria (to 3 kbar) of an andesite and basaltic andesite from western Mexico: constraints on water content and conditions for phenocryst growth: Contributions to Mineralogy and Petrology, v. 130, p. 304–319.
Nakamura, N., 1974, Determination of REE, Ba, Fe, Mg, Na, and K in carbonaceous and ordinary chondrites: Geochimica et Cosmochimica Acta, v. 38, p. 757–773.
Neuman, R. B., Palmer, A. R., and Dutro, J. T., Jr., 1989, Paleontological contributions to Paleozoic paleographic reconstructions of the Appalachians, *in* Hatcher, R. D., Jr., Thomas, W. A., and Vielle, G. W., editors, The Geology of North America, v. F-2, The Appalachian-Oucahita Orogen in the United States: Geological Society of America, p. 375–384.
Nowlan, G. S., and Neuman, R. B., 1995, Paleontological contributions to Paleozoic paleogeographic and tectonic reconstructions, *in* Williams, H., editor, Geology of the Appalachian-Caledonian Orogen in Canada and Greenland, The Geology of North America, v. F-1: Geological Society of America, p. 817–842.
O'Brien, H. G., Irving, A. J., and McCallum, I. S., 1991, Eocene potassic magmatism in the Highwood Mountains, Montana: Petrology, geochemistry, and tectonic implications: Journal of Geophysical Research, v. 96, n. B8, p. 13,237–13,260.
O'Brien, H. G., Irving, A. J., McCallum, I. S., and Thirlwall, M. F., 1995, Strontium, neodymium, and lead isotopic evidence for the interaction of post-subduction asthenospheric potassic mafic magmas of the Highwood Mountains, Montana, USA, with ancient Wyoming craton lithospheric mantle: Geochimica et Cosmochimica Acta, v. 59, p. 4539–4556.
Ogilvie, I. H., 1907, A contribution to the geology of southern Maine: Annals of the New York Academy of Sciences, v. 17, p. 519–558.
Osberg, P. H., 1978, Synthesis of the geology of the northeastern Appalachians, U.S.A.: Geological Survey of Canada Paper 78-13, p. 137–147.
Osberg, P. H., Hussey, A. M., II, and Boone, G. M., 1985, Bedrock geologic map of Maine: Maine Geological Survey Publication, Scale = 1:500,000.
Osberg, P. H., Tull, J. F., Robinson, P. R., Hon, R., and Butler, J. R., 1989, The Acadian Orogeny, *in* Hatcher, R. D., Jr., Thomas, W. A., and Viele, G. W., editors The Appalachian-Ouachita Orogen in the United States: Geological Society of America DNAG volume F-2, p. 179–232.
Pankiwskyj, K. A., 1976, Preliminary report on the geology of the Liberty 15' quadrangle and adjoining parts of the Burnham, Brooks, Belfast, and Vassalboro quadrangles in south-central Maine: Maine Geological Survey Publication 76–29.
Peccerillo, A., 1985, Roman comagmatic province (central Italy): evidence for subduction-related magmatism: Geology, v. 13, p. 103–106.
Pegram, W. J., 1990, Development of continental lithospheric mantle as reflected in the chemistry of the Mesozoic Appalachian Tholeiites, U.S.A: Earth and Planetary Science Letters, v. 97, p. 316–331.
Perini, G., Tepley, F. J., Davidson, J. P., and Conticelli, S., 2003, The origin of K-feldspar megacrysts hosted in alkaline potassic rocks from central Italy: a track for low-pressure processes in mafic magmas: Lithos, v. 66, p. 223–240.
Righter, K., and Carmichael, I. S. E., 1996, Phase equilibria of phlogopite lamprophyres from western Mexico: biotite-liquid equilibria and P-T estimates from biotite-bearing igneous rocks: Contributions to Mineralogy and Petrology, v. 123, p. 1–21.

Robinson, P., Tucker, R. D., Bradley, D., Berry, N. H., IV, and Osberg, P. H., 1998, Paleozoic orogens in New England, USA: GFF, v. 120, p. 119–148.

Rodgers, J., 1982, The life history of a mountain range – The Appalachians, *in* Hsu, K. J., editor, Mountain building processes: New York, Academic Press, p. 229–241.

Rogers, N. W., Hawkesworth, C. J., Parker, R. J., and Marsh, J. S., 1985, The geochemistry of potassic lavas from Vulsini, central Italy and implications for mantle enrichment processes beneath the Roman region: Contributions to Mineralogy and Petrology, v. 90, p. 244–257.

Royden, L. H., 1993, The tectonic expression slab pull at continental convergent boundaries: Tectonics, v. 12, p. 303–325.

Samson, S. D., Hibbard, J. P., and Wortman, G. L., 1995, Nd isotopic evidence for juvenile crust in the Carolina terrane, southern Appalachians: Contributions to Mineralogy and Petrology, v. 121, p. 171–184.

Samson, S. D., Barr, S. M., and White, C. E., 2000, Nd isotopic characteristics of terranes within the Avalon Zone, southern New Brunswick: Canadian Journal of Earth Sciences, v. 37, p. 1039–1052.

Seaman, S. J., Wobus, R. A., Wiebe, R. A., Lubick, N., and Bowring, S. A., 1995, Volcanic expression of bimodal magmatism: The Cranberry Island-Cadillac Mountain Complex, Coastal Maine: Journal of Geology, v. 103, p. 301–311.

Sisson, T. W., and Grove, T. L., 1993, Experimental investigations of the role of H_2O in calc-alkaline differentiation and subduction zone magmatism: Contributions to Mineralogy and Petrology, v. 113, p. 143–166.

Sloman, L. E., 1989, Triassic shoshonites from the Dolomites, Northern Italy: Alkaline arc rocks in a strike-slip setting: Journal of Geophysical Research, v. 94, p. 4655–4666.

Stacey, J. S., and Kramers, J. D., 1975, Approximation of terrestrial Pb isotope evolution by a two-stage model: Earth and Planetary Science Letters, v. 26, p. 207–221.

Stewart, D. B., Arth, J. G., and Flohr, M. J. K., 1988, Petrogenesis of the South Penobscot Intrusive Suite, Maine: American Journal of Science, v. 288-A, p. 75–114.

Stolz, A. J., Varne, R., Wheller, G. E., Foden, J. D., and Abbott, M. J., 1988, The geochemistry and petrogenesis of K-rich alkaline volcanics from Batu Tara volcano, eastern Sunda Arc: Contributions to Mineralogy and Petrology, v. 98, p. 374–389.

Swanson, S. E., 1977, Relation of nucleation and crystal-growth rate to the development of granitic textures: American Mineralogist, v. 62, p. 966–978.

Sun, S. S., and McDonough, W. F., 1989, Chemical and isotopic systematics of oceanic basalts: implications for mantle composition and processes, *in* Saunders, A. D., and Norry, M J., editors, Magmatism in the Ocean Basins: London, Geological Society Special Publication 42, p. 313–345.

Taylor, S. R., and McLennan, S. M., 1985, The continental crust: its composition and evolution: Oxford, United Kingdom, Blackwell Scientific Publications, 312 p.

Thirlwall, M. F., 2000, Inter-laboratory and other errors in Pb isotope analyses investigated using a Pb-207-Pb-204 double spike: Chemical Geology, Isotope Geoscience Section, v. 163, p. 299–322.

Thompson, R. N., and Fowler, M. B., 1986, Subduction-related shoshonitic and ultrapotassic magmatism: a study of Siluro-Ordovician syenites from the Scottish Caledonides: Contributions to Mineralogy and Petrology, v. 94, p. 507–522.

Thompson, R. N., Leat, P. T., Dickin, A. P., Morrison, M. A., Handry, G. L., and Gibson, S. A., 1989, Strongly potassic mafic magmas from lithospheric mantle sources during continental extension and heating: evidence from Miocene minettes of northwester Colorado, U.S.A.: Earth and Planetary Science Letters, v. 98, p. 139–153.

Tomascak, P. B., Krogstad, E. J., and Walker, R. J., 1996. Nature of the crust in Maine, USA: Evidence from the Sebago batholith: Contributions to Mineralogy and Petrology, v. 125, p. 45–59.

——— 1999. The significance of the Norumbega Fault Zone in southwestern Maine: clues from the geochemistry of granitic rocks, *in* Ludman, A., and West, D. P., Jr., editors, The Norumbega Fault System of the Northern Appalachians: Geological Society of America Special Paper, v. 331, p. 105–119.

Tomascak, P. B., Brown, M., Solar, G. S., Becker, H. J., Centorbi, T. L., and Tian, J., 2005, Source contributions to Devonian granite magmatism near the Laurentian border, New Hampshire and western Maine, USA: Lithos, v. 80, p. 75–99.

Trefethen, J. M., 1937, The Lincoln Sill: Journal of Geology, v. 45, p. 353–380.

Tucker, R. D., Osberg, P. H., and Berry, H. N., IV, 2001, The geology of a part of Acadia and the nature of the Acadian Orogeny acrosss central and eastern Maine: American Journal of Science, v. 301, p. 205–260.

Turner, S., Arnaud, N., Liu, J., Rogers, N., Hawkesworth, C., Harris, N., Kelley, S., van Calsteren, P., and Deng, W., 1996, Post-collisional shoshonitic volcanism on the Tibetan plateau: implications for convective thinning of the lithosphere and the source of ocean island basalts: Journal of Petrology, v. 27, p. 45–71.

van Staal, C. R., and de Roo, J. A., 1995, Mid-Paleozoic tectonic evolution of the Appalachian Central Mobile Belt in northern New Brunswick, Canada: Collision, extensional collapse and dextral transpression, *in* Hibbard, J. P., van Staal, C. R., and Cawood, P. A., editors, Current perspectives in the Appalachian-Caledonian Orogen: Geological Association of Canada, Special Paper 41, p. 367–389.

van Staal, C. R., Dewey, J. F., Mac Niocaill, C., and McKerrow, W. S., 1998, The Cambrian-Silurian tectonic evolution of the northern Appalachians and British Caledonides: history of a complex, west and southwest Pacific-type segment of Iapetus, *in* Blundell, D. J., and Scott, A. C., editors, Lyell: the Past is the Key to the Present: Geologic Society Special Publication 143, p. 199–242.

van Staal, C. R., Wilson, R. A., Rogers, N., Fyffe, L. R., Langton, J. P., McCutcheon, S. R., McNicoll, V., and Ravenhurst, C. E., 2003, Geology and tectonic history of the Bathurst Supergroup, Bathurst Mining Camp and its relationship to coeval rocks in southwestern New Brunswick and adjacent Maine - a synthesis, *in* Goodfellow, W. D., McCutcheon, S. R., and Peter, J. M., editors, Massive Sulfide Deposits of the Bathurst Mining Camp, New Brunswick and Northern Maine: Economic Geology Monograph 11, p. 37–60.

Vaughan, A., and Scarrow, J. H., 2003, K-rich mantle metasomatism control of localization and initiation of lithospheric strike-slip faulting: Terra Nova, v. 15, p. 163–169.

West, D. P., Jr., 1999, Timing of displacements along the Norumbega fault system, south-central and south-coastal Maine, *in* Ludman, A., and West, D. P., Jr. editors, Norumbega fault system of the northern Appalachians: Geological Society of America Special Paper 331, p. 167–178.

——— 2004, Bedrock geology of the Washington 7.5′ quadrangle, Maine: Maine Geological Survey Map 04-28: Scale = 1:24,000.

West, D. P., Jr., and Hubbard, M. S., 1997, Progressive localization of deformation during exhumation of a major strike-slip shear zone: Norumbega fault zone, south-central Maine: Tectonophysics, v. 273, p. 185–201.

West, D. P., Jr., and Peterman, E. M., 2004, Bedrock geology of the Razorville 7.5' quadrangle, Maine: Maine Geological Survey Map 04-29, Scale = 1:24,000.

West, D. P., Jr., Guidotti, C. V., and Lux, D. R., 1995, Silurian orogenesis in the western Penobscot Bay region, Maine: Canadian Journal of Earth Sciences, v. 32, p.1845–1858.

West, D. P., Jr., Senese, M. A., and Sterrett, J. B., 2000, Structural geology and tectonics of Silurian-Devonian terrane accretion in south-central Maine, *in* Yates, M. G., Lux, D. R., and Kelley, J. T., editors, Guidebook for Field Trips in Coastal and East-Central Maine: New England Intercollegiate Geological Conference Guidebook, p. 107–128.

West, D. P., Jr., Beal, H. M., and Grover, T. W., 2003, Silurian deformation and metamorphism of Ordovician arc rocks of the Casco Bay Group, south-central Maine: Canadian Journal of Earth Sciences, v. 40, p. 887–905.

West, D. P., Jr., Coish, R. A., and Tomascak, P. B., 2004, Tectonic setting and regional correlation of Ordovician metavolcanic rocks of the Casco Bay Group, Maine: evidence from trace element and isotope geochemistry: Geological Magazine, v. 141, p. 125–140.

Whalen, J. B., Jenner, G. A., Longstaffe, F. J., and Hegner, E., 1996a, Nature and evolution of the eastern margin of Iapetus: geochemical and isotopic constraints from Siluro-Devonian granitoid plutons in the New Brunswick Appalachians: Canadian Journal of Earth Sciences, v. 33, p. 140–155.

Whalen, J. B., Fyffe, L. R., Longstaffe, F. J., and Jenner, G. A., 1996b, The position and nature of the Gander-Avalon boundary, southern New Brunswick, based on geochemical and isotopic data from granitoid rocks: Canadian Journal of Earth Sciences, v. 33, p. 129–139.

Wiebe, R. A., 1993, The Pleasant Bay layered gabbro-diorite, coastal Maine: ponding and crystallization of basaltic injections into a silicic magma chamber: Journal of Petrology, v. 34, p. 461–489.

——— 1994, Silicic magma chambers as traps for basaltic magmas: The Cadillac Mountain Intrusive Complex, Mount Desert Island, Maine: Journal of Geology, v. 102, p. 423–437.

Wiebe, R. A., Monon, M. R., Hawkins, D. P., and McDonough, W. F., 2004, Late stage mafic injection and thermal rejuvenation of the Vinalhaven granite, coastal Maine: Journal of Petrology, v. 45, p. 2133–2153.

Williams, H. M., Turner, S. P., Pearce, J. A., Kelley, S. P., and Harris, N. B. W., 2004, Nature of the source regions for post-collisional, potassic magmatism in southern and northern Tibet from geochemical variations and inverse trace element modeling: Journal of Petrology, v. 45, p. 555–607.

Wilson, M., 1989, Igneous Petrogenesis: A global tectonic approach: London, Unwin Hyman, 466 p.

Wyllie, P. J., and Sekine, T., 1982, The formation of mantle phlogopite in subduction zone hybridization: Contributions to Mineralogy and Petrology, v. 79, p. 375–380.

Yang, J., Chung, S., Wilde, S. A., Wu, F., Chu, M., Lo, C., and Fan, H., 2005, Petrogenesis of post-orogenic syenites in the Sulu Orogenic belt, East China, goechronological, geochemical, and Nd-Sr isotopic evidence: Chemical Geology, v. 214, p. 99–125.

Zhang, H. F., Sun, M., Zhou, X. H., and Ying, J. F., 2005, Geochemical constraints on the origin of Mesozoic alkaline intrusive complexes from the North China Craton and tectonic implications: Lithos, v. 81, p. 297–317.